U.S. Officials Only

CONFIDENTIAL

SECURITY INFORMATION

CPYRGHT

CENTRAL INTELLIGENCE AGENCY

INFORMATION REPORT

25X1A

[redacted]

COUNTRY USSR

SUBJECT Review of Five Soviet Metallurgical Texts

PLACE ACQUIRED (BY SOURCE) 25X1A

DATE ACQUIRED (BY SOURCE) [redacted]

DATE [redacted]

25X1X

SOURC[redacted]

Available on loan from CIA Library are summaries of the following five Soviet texts:

a) Principles of the Study of Metals and Heat Treatment, 170 pp, Government Scientific - Technical Publishing House of Machine Industry Literature, undated.

(Reviewer's Remarks: There are a few data (mentioned in this review) which would probably be of some interest but, in general, the material presented in this book is well known to US metallurgists.)

b) Induction Hardening, (Termitcheskaia Obrabotka Stali pri Inductsionnom Nagreve), by J N Kidin, 316 pp, Government Scientific - Technical Publishing House of Ferrous and Non-Ferrous Metallurgy, Moscow, 1950.

(Reviewer's Remarks: In the Reviewer's opinion this book is a valuable contribution to our knowledge on Induction Hardening. It covers thoroughly different problems involved in this process. Most of the conclusions drawn by the author are supported by results of his own extensive investigations. The author demonstrates very well that there are two main factors governing induction hardening processes. These factors are: temperature and heating rate. It may be noted, however, that many of the photomicrographs are not distinct enough and no details are given as to etching reagents and magnifications used.)

c) Metallurgy of Steel, Open Hearth Process. (Metallurgiia Stali Martenovskii Process), K G Trubin and G N Oyks, 763 pp, Government Scientific Technical Publishing House of Ferrous and Non-Ferrous Metallurgy, Moscow, 1951.

(Reviewer's Remarks: Some paragraphs of the book are too sketchy and not clear enough, whereas others are unduly lengthy and contain too many unnecessary details, theoretical discussions and repetitions. In general,

U.S. Officials Only

CONFIDENTIAL

SECURITY INFORMATION

DISTRIBUTION	STATE	X	ARMY	X	NAVY	X	AIR	X	FBI		ATIC	X	AEC X

This report is for the use within the USA of the Intelligence components of the Departments or Agencies indicated above. It is not to be transmitted overseas without the concurrence of the originating office through the Assistant Director of the Office of Collection and Dissemination, CIA.

Approved For Release 2001/07/31 : CIA-RDP80-00809A000500170204-4

[redacted]

the material presented in this text book is fairly well known to US Metallurgists. Nevertheless some parts of the book selected by the reviewer would probably be of some interest. It is very significant that, evidently for political reasons, in their discussion on crystallization of steel, no mention was made by the authors of the work of Colonel N T Belaiew, the ablest pupil of Prof Tchernoff. In referring to his work Sauveur ("The Metallography and Heat Treatment of Iron and Steel", Albert Sauveur, Second Edition 1918, page 208) stated that "we are indebted to Colonel Belaiew more than to any one else for our knowledge of the crystallization of steel".

d) Iron-Chromium-Alluminum Alloys by I I Kornilov of the Institute of General and Inorganic Chemistry, Laboratory of the Iron Alloys. Published by Academy of Science, Moscow 1945.

(Reviewer's Remarks: This book should be of interest to US readers, particularly to those thoroughly familiar with the subject. The book contains 51 tables and 154 figures. A great majority of them would require a lengthy description which is impossible to make in a short abstract. It is suggested, therefore, that the reader consult the text as indicated in the present review. It is considered that magnification of some photomicrographs is not adequate; it is not high enough for a correct interpretation of the structures discussed.)

e) Flakes In Steel (Flokeni v Stali), 332 pp, by V S Doubovoi, Government Scientific-Technical Publishing House of Ferrous and Non-Ferrous Metallurgy, Moscow, 1950.

(Reviewer's Remarks: This book is difficult to read because of an excessive number of details which are not well coordinated. The arguments against the hydrogen theory (that hydrogen is the only factor responsible for the presence of flakes) are somewhat conflicting and not entirely convincing. However, some data presented by the author and described in this review should be of interest to US readers.)_7

- end -

Approved For Release 2001/07/31 : CIA-RDP80-00809A000500170204-4

25X1A

[redacted]

PRINCIPLES OF THE STUDY OF METALS AND HEAT TREATMENT.

Book 170 pages, Government Scientific- Technical Publishing House of Machine Industry Literature.

The book is divided into 10 parts. It concerns only the iron-carbon alloys.

Part 1 - A brief outline of physical metallurgy, pp. 6-19.

Steel making processes classification and structure of steel are briefly outlined. The iron-carbon constitutional diagram shown in fig 5, p.14 is an outdated diagram. This part is of no interest to American metallurgists.

Part 2 - Principles of heat treatment of steel, pp. 20-58.

This part contains common information on quenching, tempering, induction surface hardening, nitriding, cyaniding, carbonitriding and heat treating furnaces.

Part 3 - Metals used in the manufacture of automotive parts, pp 59-61.

Common knowledge.

Part 4 - Heat treatment of forgings, pp 62-70.

Annealing and normalizing of forged pieces and their control by Brinell hardness and metallographic examinations are very briefly discussed.

Part 5 - Quenching of different articles, pp 71-87.

Quenching of hub-nave (fig.35, p.72), camshaft (fig.38, p.74), crankshaft, driving gears (fig.47, p.82), piston pins (fig. 50, p.87) is described.

A general view of the assembly used for quenching rolls is shown in fig.30, p.77 but no detailed description is given. The quenching press for quenching gears is shown in fig. 49, p.84. It is equipped with two pneumatic cylinders for the lower and upper dies. The lower part of the press has a reservoir filled with oil. A hot gear with its teeth up is placed on the lower die and the upper die is pushed down, so that gear is clamped between these dies. Next, the dies and gear are immersed into oil by means of air pressure of the upper cylinder. The oil enters under pressure though the openings No.1 and circulates between the gear's teeth.

Part 6 - Quenching from surface heating, pages 88-96.

The high frequency induction heating and flame hardening are briefly outlined. It is stated that the best results in an induction heating practice are obtained with steels containing 0.40 to 0.45% C. The hardened layer of quenched article consists of two zones, zone made of martensite and troostite-martensite and a transition zone. The depth of the first zone should constitute at least 75% of the total depth of the hardened layer. In induction hardening, the position of an article in the induction furnace is of great importance. The hardened layer of the cylindrical article should be concentric to its surface and of uniform depth. To obtain this, an article should be placed in the furnace concentrically

Approved For Release 2001/07/31 : CIA-RDP80-00809A000500170204-4

with respect to the induction coil, otherwise one may expect result similar to that illustrated in fig.51, p.92, i.e. excentric position and ununiformity ~~uniformity~~ in depth of the hardened layer. Effect of a crack on hardened layer is demonstrated in fig. 54, p.92.

Part 7 - Tempering, pp.97-104

Mechanical properties of tempered steels depend upon the temperature, duration of tempering operation and, for certain alloy steels, upon the rate of cooling.

Fig. 61, p.101, shows the effect of tempering temperature on the Rockwell hardness of steels containing 0.20, 0.35 and 0.60% C.

The influence of temperature on the impact toughness is presented in fig. 62, p.101. The rate of heating in the liquid media is 2 to 3 times greater than in the gaseous media. Therefore the duration of tempering in a liquid medium is smaller as compared with a gaseous medium. For plain carbon steels, the cooling rate of a tempered article has practically no effect on its mechanical properties. For the alloy steels (nickel-chromium, chromium manganese, chromium and some other steels) the impact toughness decreases with a decrease of cooling rate. This relation is illustrated in fig. 64, p.103 for steel containing 0.3% C, 1.47% Cr and 3.6% Ni. The tempering temperatures in °C are plotted on abscissa and impact toughness kg/cm^2 on ordinate.

Approved For Release 2001/07/31 : CIA-RDP80-00809A000500170204-4

Approved For Release 2001/07/31 : CIA-RDP80-00809A000500170204-4

Solid line refers to fast cooling and broken line to slow one.

Part 8 - Carburization, pp. 105-129.

The pack and gas carburizing process and also heat treatment of the case hardened machine parts are described. Two types of the carburizing compounds used in one Russian plant are given in table 5, p.110.

Table 5

Type	Barium carbonate %	Sulphur maxim. %	Calcium Carbonate %	Silica maxim. %	Alumina maxim %	Water maxim. %
A	20-25	0.06	3.5	0.5	0.5	5.0
B	20-25	0.10	5.0	1.5	—	5.0

The boxes employed for carburization should be constructed in such a manner that for a given volume their surface exposed for heating is the maximum. They should be made of a heat-resisting alloy. Rate of heating in the boxes during carburization is given in fig. 71, p.114.
Temperatures in °C are plotted on ordinate and time in hrs. on abscissa. Solid line evidently (no explanation is given) represents temperatures measured in the middle part of the box and broken line near its surface. The required temperature is reached by the article subjected to carburization only after 4 to 5 hrs.
At the present time, gas carburization finds a wide application. For this purpose a mixture of gases produced from kerosene

Approved For Release 2001/07/31 : CIA-RDP80-00809A000500170204-4

Approved For Release 2001/07/31 : CIA-RDP80-00809A000500170204-4

by pyrolisis and cracking processes is of particular use. Equipment used for pyrolisis and cracking processes is shown in fig. 72:72a p.117 - General view; 72b p.118 - Side View; 72C, p. 119 - Low part of equipment.

In figures 73, p.122 and 74, p.123 are shown equipment for purification and drying of gases and a muffle furnace for gas carburization (longitudinal section)

Part 9 - Cyaniding of machine parts, pp. 130-148.

Cyaniding is used in both, low and medium carbon steels. Cyaniding mixtures used in Russian plants are given in table 7, p.132. The first column of this table indicates the grade, the second, third and fourth columns - percents of sodium cyanide, sodium carbonate and sodium chloride respectively. The mixture containing 75% cyanide is considered as very practical.

Influence of sodium cyanide concentration on depth of case in mm. in 40 x steel (C, 0.35 - 0.45; Mn, 0.50 - 0.80, Si, 0.17 - 0.37; Cr, 0.80 - 1.10%) at different °C is shown in fig. 81, p.133. Duration of cyaniding was 40 minutes. Sodium cyanide concentration is plotted on abscissa and depth of case in mm. on ordinate.

Effect of temperature on case depth in mm. is presented in fig. 82, p.134. Sodium cyanide concentration was 20% and duration of process 45 minutes.

Temperatures °C are plotted on abscissa and case depth on ordinate. The type of steel used in these experiments is not

Approved For Release 2001/07/31 : CIA-RDP80-00809A000500170204-4

Approved For Release 2001/07/31 : CIA-RDP80-00809A000500170204-4

mentioned. It is assumed that it was the same 40 x steel.

Effect of temperature and duration of heating on depth of case in 20 x steel (C, 0.15 - 0.25; Mn, 0.30 - 0.60; Si, 0.17 - 0.37; Cr, 0.70 - 1.00) is shown in fig.83. Sodium cyanide concentration was 20%. Duration in min. is plotted on abscissa and case depth in mm. on ordinate.

Same relationship but for steel 40 X (Chemical analysis of this steel is given above) is shown in fig. 84, p.135. Steels investigated were 20 X, 40 X and 40. Chemical analysis of steels 20 X and 40 X were already mentioned. Chemical analysis of steel 40 is as follows:

C, 0.30 - 45; Mn, 0.50 - 0.80; Si, 0.17 - 0.37; S max. 0.045; and P max 0.045% .

Part 10 - Heat treatment of springs, discs and couplings pp. 149-152

This part is of no particular interest.

BIBLIOGRAPHY, p.152

There are 12 references, all Russian Publications.

APPENDIX, pp. 153-170

There are 10 tables. In table 1 are given different types of steels, their chemical analyses, Brinnel hardness, tensile strength in kg/mm^2 and % elongation.

Table 2, pp 154, 155 shows different types of steel, their chemical analyses and Brinell hardness for both, annealed and unannealed steels.

Approved For Release 2001/07/31 : CIA-RDP80-00809A000500170204-4

Approved For Release 2001/07/31 : CIA-RDP80-00809A000500170204-4

Table 3, p.156: A - Tensile strength, elongation and yield point values of 8 types of the plain carbon steels. B - Chemical analysis of those steels.

Table 4 - Heat treatment and characteristics of the common structural steels.

Tables 5 to 8 inclus. - Different types of spring and wire steels, their chemical analysis, heat treatment, tensile strength and hardness.

Table 10 - Brinell and Rockwell hardness and corresponding tensile strength values of some plain carbon, chromium and nickel-chromium steels.

Reviewer's remarks:

There are a few data (mentioned in this review) which would probably of some interest but, in general, the material presented in this book is well known to American metallurgists.

25X1X

[redacted]

May 19, 1953

Approved For Release 2001/07/31 : CIA-RDP80-00809A000500170204-4

Approved For Release 2001/07/31 : CIA-RDP80-00809A000500170204-4

Table 3, o.156: A - Tensile strength, elongation and yield point values of 8 types of the plain carbon steels. B - Chemical analysis of those steels.

Table 4 - Heat treatment and characteristics of the common structural steels.

Tables 5 to 8 inclus. - Different types of spring and wire steels, their chemical analysis, heat treatment, tensile strength and hardness.

Table 10 - Brinell and Rockwell hardness and corresponding tensile strength values of some plain carbon, chromium and nickel-chromium steels.

Reviewer's remarks:

There are a few data (mentioned in this review) which would probably of some interest but, in general, the material presented in this book is well known to American metallurgists.

25X1X

[redacted]

May 19, 1953

Approved For Release 2001/07/31 : CIA-RDP80-00809A000500170204-4

Approved For Release 2001/07/31 : CIA-RDP80-00809A000500170204-4

25X1A 2.

[redacted]

Doc. 6

Approved For Release 2001/07/31 : CIA-RDP80-00809A000500170204-4

Approved For Release 2001/07/31 : CIA-RDP80-00809A000500170204-4

INDUCTION HARDENING. (Termitcheskaia obrabotka stali pri inductsionnom nagreve), J.N.Kidin, book 316 pages, Government Scientific-Technical Publishing House of Ferrous and Non-Ferrous. Metallurgy, Moscow, 1950.

The book is divided into 10 parts.

Part 1 - Methods of Surface hardening of steel articles, pages 13 to39.

There are three basic methods of hardening

1. Thormo-chemical treatment
2. Surface hardening by external source of heating
3. Surface hardening by internal source of heating.

In the thermo-chemical treatment the surface layer of an article is saturated with carbon, nitrogen, chromium or some other elements and the article is then heat treated. In this case, the steel article is heated through and it is very difficult to control the properties throughout its cross section. Cementation 1.0, to 1.5 mm. deep requires 10-15 hrs.

Surface hardening may be produced by the use of oxyacetylene or some other flame, of a liquid bath, or electrolyte (Yasnogorodsky's method). Flame hardening may be successfully applied to steel when the contents of the different elements are within the following limits: C, 0.30 - 0.70%; Mn, 0.60 - 1.60%; Si, 0.20 - 1.50%; Cr, 0.20 - 1.75%; Ni, 0.30 - 3.50%; Mo, 0.15 - 0.30%.

However, flame hardening is mostly applied to a plain carbon steel containing 0.45% C.

Surface hardening of steel is sometimes carried out in molten lead

Approved For Release 2001/07/31 : CIA-RDP80-00809A000500170204-4

Approved For Release 2001/07/31 : CIA-RDP80-00809A000500170204-4

which, being heated to 800° - 850°C, has a very high coefficient of heat conductivity.

In the electrolyte method developed by Yasnogorodsky the lead plate (anode) and steel rod (cathode) are immersed into sodium chloride or some other electrolyte solution. A high tension electric current passing through the bath forms a hydrogen envelope around steel rod. This envelope is quickly heated to a high temperature (about 2000°C) and transfers its heat to the steel rod. When the temperature at the surface of steel rod is somewhat above the Ac_3 point the power is cut off, the hydrogen envelope disappears and the steel rod is quenched in the electrolyte.

A contact method (surface hardening using an internal source of heating) is described as follows: a steel article (cylinder) is placed between the centers of a lathe. A small copper roller (fig. 7, p.26) rigidly secured in the slide-rest of the machine is brought into contact with the steel cylinder and closes the electrical circuit of current passing trough the steel cylinder to the copper roller.

When the lathe is put in operation the steel cylinder and roller start to rotate and the copper roller is traversed automatically parallel to the steel cylinder. Since the contact area between the roller and cylinder is very small, the current density is greatly increased at that point. As soon as the heated portion of the steel cylinder comes out of contact with the roller it is sprayed with a cooling liquid. With this installation the temperature of the surface layer 0.06-0.1 mm thick of steel cylinder was found to be about 450°C and this layer was not hardened. The temperature of the next layer was found to be

Approved For Release 2001/07/31 : CIA-RDP80-00809A000500170204-4

Approved For Release 2001/07/31 : CIA-RDP80-00809A000500170204-4

between Ac_1 and Ac_3 points and this layer was not fully hardened, its structure being made of martensite and ferrite. The following to that layer was heated above the Ac_3 point and it was fully hardened (martensitic structure). The core of the steel cylinder remained unaffected by the treatment and showed its original structure.

Part 2 - Fundamental characteristics of Induction heating, pp. 40-63

This theoretical discussion does not seem to warrant abstraction.

Part 3 - Phase transformation in steel heated by external source of heat. pp. 14 - 80.

It is well established that the formation of austenite from ferrite-cementites is by a process of nucleation and growth. The nucleation occurs at the ferrite-carbide grain boundary. The process of austenite formation mostly depends upon the structure of pearlite. The highest rate of transformation into austenite is observed for the fine lamellar pearlite. The greater rate of heating, the higher is the temperature of the beginning of the pearlite→ austenite transformation and the shorter is the period of this transformation. The rate of formation of austenite grains depends to a great extent upon the temperature. This is illustrated in fig.35, p.72 and may be seen from the following data:

Temp. °C ___	740	760	780	800
Rate of formation in mm^3/sec. ___	$2.28.10^3$	11.10^3	$51.5.10^3$	$61.6.10^4$

The rate of growth of austenite grains is inversely proportional to the pearlite spacing. This is illustrated in fig.37 p.75, where

Approved For Release 2001/07/31 : CIA-RDP80-00809A000500170204-4

Approved For Release 2001/07/31 : CIA-RDP80-00809A000500170204-4

pearlite spacings in microns are plotted on abscissa and rates of growth in mm/sec. x 10^3 on ordinate. In fig. 38, p.75, logarithms of rate of growth in mm/sec. are plotted (abscissa) versus temperatures of isothermic transformation (ordinate) for pearlite (spacing 0.6μ and troostite (spacing 0.1μ).

The number of grains N per 1 mm^2 may be determined from formula

$$N = 1.01\left(\frac{n}{g}\right)^{1/2}$$

where n - rate of nucleation

and g - rate of austenite grain growth.

It was concluded that the greater the rate of heating, the finert the grains produced.

For the same rate of heating, temperature and form of carbides, the process of nucleation and growth of austenite depends to a great extent upon the carbon content in steel. The time necessary for completion of a certain definite part of process $\tau = \frac{K}{C}$ where τ is time, K - constant and C - carbon concentration. This relation is illustrated in fig's 40 and 41, p.78, where time in minutes is plotted on abscissas and temperatures in °C on ordinates. Fig. 40 refers to a plain carbon steel and Fig.41 to steel containing 2% Cr.

It is well known that the position of the Ac_1 point depends upon the rate of heating. Svetchnikoff and Gridneff demonstrated that there is a critical rate of heating beyond which it practically has no effect on the Ac_1 point. This critical rate was found to be approximately 200°-250°C per min.(4°C per sec.) The data obtained by Gridneff are illustrated in fig.42, p.79, where time is plotted on

Approved For Release 2001/07/31 : CIA-RDP80-00809A000500170204-4

Approved For Release 2001/07/31 : CIA-RDP80-00809A000500170204-4

absicsa and temperature on ordinate. It may be seen that with rates of heating of 30°, 80°, 140°, 320° and 2000°C per min. the Ac_1 points were respectively 735°, 745°, 770°, 775° and 775°C.

Part 4 - Phase transformation in steel heated by an internal source. pp. 80-118.

In the discussion below under "Internal Source of Heating" is meant "Induction Heating".

Induction heating involves a very rapid heating of an article (steel) by induced alternating currents to quenching temperature. The hardening by induction methods depends upon the electrical characteristics of the generator and the induction oscillator as well as the metallurgical characteristics of the steel.

Some investigators limited themselves to recording the electrical data and time of heating. Some related surface hardness and depth of hardening to the energy (KW. sec) consumed ignoring the most important factor - temperature (quenching temperature).

It is easy to show that quite different results than those reported by different investigators could be obtained on using other generator and heating outfits. It is to be borne in mind that only the portion of energy absorbed by the steel article has an affect on its heating. Even when using the same generator but other induction oscillator the heating process may be different. In refering now to other factor, i.e. rate of heating it may be noted that in many cases the rate of an induction heating is greater below the Curie point (below it iron is magnetic and above it is not, reviewer's remark)

Approved For Release 2001/07/31 : CIA-RDP80-00809A000500170204-4

Approved For Release 2001/07/31 : CIA-RDP80-00809A000500170204-4

than above it. In some cases this phenomenon is more pronounced than in others. Therefore for the same total time of heating cycle one may obtain different results on account of difference in the rates of heating of steel articles between the Curie point and the quenching temperature. This is illustrated in fig. 45, p.87, where time is plotted on abscissa and temperature on ordinate. The total time in both cases is the same. t_1 is the quenching temperature. Although the total time of heating is the same the time periods of heating between the Curie point and the quenching temperature are different (a and b). In the induction hardening as in a regular hardening process, the heating temperature is a very important factor. In the induction hardening another very important factor is the rate of heating in the phase transformation zone. In view of the very fast heating, temperature measurement in the induction method is extremely difficult. Quite satisfactory results were obtained with an optical pyrometer with an accuracy within 10-15°C. Fig. 49, p.92 shows the Losinsky's automatic photopyrometric installation. During heating the photoelectrical pyrometer (equipped with photocell) 3 is directed on specimen 1 held by frame 2. Latch 5 connected with an electromagnet supports frame 2 until the temperature of the specimen reaches a given temperature. At that point the generator is automatically cut off and the specimen plunges into a cooling liquid.

The author believes that when determining the rate of induction heating it is necessary to calculate the rate of heating for zones located below and above the Curie point (ab. 770°C). From the phase transformation point of view, the second zone (above Curie point)

Approved For Release 2001/07/31 : CIA-RDP80-00809A000500170204-4

Approved For Release 2001/07/31 : CIA-RDP80-00809A000500170204-4

is most important.
Based on the above two factors, temperature and rate of induction heating, the author could determine the effect of absorbed energy without calculation.

When the electric current passes through a conductor consisting of one phase, it's flow is uniform throughout the I - I section (Fig. 50a, p.103) and its density is determined with reference to the whole section. If the conductor consists of two phases having different electroconductivities the current flows in the direction shown by II - II line (same fig.50a). In that section there are carbides inclusions possessing a very high electrical resistance. The distribution of current density across section II - II may be schematically illustrated as is given in fig.50b, p.103.

It is extremely difficult to determine at which conditions and how the phase transformations take place in the induction hardened steels. At the present time, it is only possible to surmise this mechanism on the basis of the properties and structures observed in the quenched specimens. There is a belief that an increase in the current density along the ferrite-carbide boundary, characteristic to induction heating, leads to a formation of the homogeneous solid solution. However the photomicrograph presented by Martin and Wiley (Induction hardening of Plain Carbon Steels: A Study of the Effect of Temperature, Composition, and Prior Structure on the Hardness and Structure after Hardening, D.L.Martin and Florence E.Wiley, Trans. Amer. Soc. for Metals, Vol.34, 1945, pp. 351-396) is a ~~clever~~ clear

Approved For Release 2001/07/31 : CIA-RDP80-00809A000500170204-4

Approved For Release 2001/07/31 : CIA-RDP80-00809A000500170204-4

demonstration of heterigeneity of martensite observed in the induction 0.8% C steel. This electron micrograph (x 9000), reproduced here in fig. 56, p.110, shows the large undissolved carbide in the pearlite surrounding it. The heterogeneity of the cored martensite is quite clear in this micrograph.

The temperature at which the rate of transformation is maximum is not the Ac_3 point but the temperature designated by the author as the Aca point. The rate of transformation at which the process progresses at different temperatures in the regular and induction heatings is illustrated in fig. 57, p.112, where the temperatures are plotted on abscissas and the rate of transformation in % on ordinates. Curve 1 refers to a regular hardening and curve 2 to an Induction hardening. Aca - temperature at which transformation progresses with a maximum speed.

X ray examination indicates that in steel containing 0.75% C, with the rate of heating 100°- 120°C per sec., complete solution of carbon is attained at approximately 920°C which is 150°- 160°C higher than Ac_3 temperature for conventional heating methods. For 1.08% C steel and rate of heating about 75°C per sec, complete solution is reached at 900°C, i.e. about 140°C above the Ac_m point with conventional rate of heating.

Part 5 - Effect of Induction Hardening on the Structure of Steel, pp. 119-157

In table 2, p.120 are given chemical analyses of different types of the plain carbon and alloy steels used in this investigation.

Approved For Release 2001/07/31 : CIA-RDP80-00809A000500170204-4

Approved For Release 2001/07/31 : CIA-RDP80-00809A000500170204-4

The samples employed were 10 - 12 mm. diam. and 100 - 120 mm. long. The effect of temperature and rate of heating on the structure and hardness was studied. Determination of surface hardness (Rc) was made on Rockwell apparatus, whereas hardness across the section (Hv) was measured on Vickers hardness tester with 5 kg. load.
Fig's 59-64, p. 122 and 123 and 66-70, pp. 123 and 124 show the structures of steels, types 40 and 50, for different quenching temperatures, the rate of heating being 380° - 400° C per sec. The Rockwell hardness Rc numbers for different quenching temperatures are shown in fig. 71, p.125, where temperature is plotted on abscissa and hardness on ordinate. On the basis of the results above, the following optimum quenching temperatures were recommended by the author: 900° - 940°C for steel type 40; 880° - 920°C for steel 45; 860° - 900° C for steel 50 and 940° - 980°C for steel 40 x, the rate of heating in these cases being 380° - 400°C per sec.

Fig's 72-75, p.127 illustrate the structural changes of steel type 40 with an increase in the rate of heating, the quenching temperature remaining constant, 960°C.
Fig. 76, p.128 shows the structure of same steel but heated conventionally and quenched from 960°C. This is shown only for comparison since the author realizes that this temperature is unusual quenching temperature for the structural steel conventionally heated.
Surface hardness (Rc) versus the rate of heating of steel 40 is presented in fig.77, p.128, where rate of heating is plotted on abscissa and Rc on ordinate.

Approved For Release 2001/07/31 : CIA-RDP80-00809A000500170204-4

Approved For Release 2001/07/31 : CIA-RDP80-00809A000500170204-4

Fig's 78 and 79 illustrate structures of steels 40 and 50 not completely hardened. The quenching temperature and rate of heating were respectively 960°C and 900°C per sec.
This shows that not only the quenching temperature but also rate of heating may be responsible for an uncomplete hardening.
Fig's 85-89, pp. 134 and 135 and 90-93, pp. 135 and 136 show structures of Y7 and Y10 plain carbon tool steels observed for different quenching temperatures (725, 920, 1000, and 1200°C) and constant rate of heating of 380-400°C per sec. Fig.94, p.136 represents the change in hardness Rc of these steels with an increase in quenching temperature.

In the study of the effect of the rate of heating on the structure and hardness of a high carbon steel, the rates of heating ranged from 40° to 700°C per sec., the quenching temperature being 920°C. The structures observed are shown in fig's 95-97, p.138 for steel Y7 and fig's 98-100, pp. 138 and 139 for steel Y10.
The change in the surface hardness with an increase in the rate of heating is presented in fig. 101, p.139. Fig. 102 shows the hardness penetration curves where Hv hardness (plotted on ordinates) was taken on a cross section at different distances (abscissas) from the surface for Y10 steel heated at different speeds.
It may be seen that there was a small but steady increase in the surface hardness Rc with an increase of the rate of heating.
With moderate rates of heating (85° - 210°C per sec.) not much change was observed in the hardness Hv along the cross section of a steel specimen. However at the higher rates (410° - 700°C per sec.) there was a considerable drop in hardness at points located only 2mm.

Approved For Release 2001/07/31 : CIA-RDP80-00809A000500170204-4

Approved For Release 2001/07/31 : CIA-RDP80-00809A000500170204-4

Fig's 78 and 79 illustrate structures of steels 40 and 50 not completely hardened. The quenching temperature and rate of heating were respectively 960°C and 900° C per sec.
This shows that not only the quenching temperature but also rate of heating may be responsible for an uncomplete hardening.
Fig's 85-89, pp. 134 and 135 and 90-93, pp. 135 and 136 show structures of Y7 and Y10 plain carbon tool steels absorved for different quenching temperatures (725, 920, 1000, and 1200°C) and constant rate of heating of 380-400°C per sec. Fig.94, p.136 represents the change in hardness Rc of these steels with an increase in quenching temperature.

In the study of the effect of the rate of heating on the structure and hardness of a high carbon steel, the rates of heating ranged from 40° to 700° C per sec., the quenching temperature being 920° C. The structures absorved are shown in fig's 95-97, p.138 for steel Y7 and fig's 98-100, pp. 138 and 139 for steel Y10.
The change in the surface hardness with an increase in the rate of heating is presented in fig. 101, p.139. Fig. 102 shows the hardness penetration curves where Hv hardness (plotted on ordinates) was taken on a cross section at different distances (abscissas) from the surface for Y10 steel heated at different speeds.
It may be seen that there was a small but steady increase in the surface hardness Rc with an increase of the rate of heating.
With moderate rates of heating (85° - 210°C per sec.) not much change was observed in the hardness Hv along the cross section of a steel specimen. However at the higher rates (410° - 700° C per sec.) there was a considerable drop in hardness at points located only 2mm.

Approved For Release 2001/07/31 : CIA-RDP80-00809A000500170204-4

Approved For Release 2001/07/31 : CIA-RDP80-00809A000500170204-4

below the surface. Therefore, very high rates of heating are not desirable for high carbon steels.

In the investigation of chromium (III X 9 and III X 15 types), chromium-tungsten-manganese (type X BГ) and chromium-silicon (type 9XC) steels, the temperatures ranged from 800° to 1300° C. The heating rate was 600° C per sec. for steels III X 9 and III X 15. For steels XBГ and 9XC it ranged from 50° to 700° C per sec. The structures observed for steel III 15 are illustrated in fig's 103-107 pp.141 and 142.

With an increase in temperature there is no significant change in the number of carbides but there is some decrease in their size. The matrix consists of an extremely fine martensite (concealed martensite). The hardness of this structure is very high, 68-69 Rc. At a heating rate of 600° C per sec., complete solution of carbides is obtained only at temperature of 1040° C.

(Reviewer's remark: Reference may be made to James P. Poynter's paper on "Metallurgical Characteristics of Induction - Hardened Steel, Trans. Amer. Soc. for Metals, Vol.36, 1946, pp. 165-209. Poyntor found that the spheroidized specimens (carbide particles large) do not respond as readily to induction heating. His microscopic examination showed that all the carbide particles near the surface temperature of 1900° F (1040° C) is reached).

At somewhat higher temperatures, the matrix consists of a fine needle martensite. With still further increase in temperature the martensite needles become larger and there appears a retained

Approved For Release 2001/07/31 : CIA-RDP80-00809A000500170204-4

Approved For Release 2001/07/31 : CIA-RDP80-00809A000500170204-4

austenite. The hardness of such structure is not over 61 Rc. The hardness - temperature relation for steels III X 15, III X 9 and XBГ is presented in fig.108, p.143. The rate of heating is 600°C per sec., the temperatures are plotted on abscissas and surface hardnesses Rc on ordinates.

Fig's 109 - 113 and 114 - 116 show the effect of the rate of heating (ranging from 40° to 600°C) on the structure of steels III x 15 and III x 9 quenched at 960°C. With slow heating, the structure of steels consists of a coarse martensite. In steels III X 15 and III X 9 the needle structure is retained until a heating rate of 125° per sec. is reached.

For steels XBГ the needles are still noticed at a heating rate of 185°C per sec. With a further increase in the rate of heating, the needles disappear and the structure consists of an extremely fine martensite (concealed crystalline structure) and a great number of carbides.

As it is shown in fig. 117, p.147, the maximum surface hardness values Rc for those steels quenched from 960°C was obtained with a heating rate of 500°C per sec. The transverse hardness Hv (ordinates) for different distances (in mm, abscissas) from the surface are presented in fig. 118, p.147.

Graphs given in fig's 119, 120 and 121 pp.148 and 149 demonstrate the effect of quenching temperature, at which a complete hardening is secured, and the rate of induction heating on the surface hardness Rc. The higher is the rate of heating, the higher is the temperature at which full hardening results are secured. The induction hardening conducted with the high rates

Approved For Release 2001/07/31 : CIA-RDP80-00809A000500170204-4

Approved For Release 2001/07/31 : CIA-RDP80-00809A000500170204-4

of heating produces the most dispersed structure possessing the maximum hardness.

In discussing the effect of initial microstructure on the structure of an induction hardened steel the author considers the results obtained by different investigators, among them those reported by D.L.Martin and Florence E.Wiley in their paper mentioned above.

In the 0.8% C steel, the austenitizing process proceeds at a greater speed if the initial structure is not coarse but fine pearlite. The most favorable initial structure for induction hardening is sorbite. With this structure, the highest surface and penetration hardenesses may be secured. The effect of initial structure is less noticeable with high quenching temperatures.

Part 6 - Mechanical Properties of the Induction Hardened Steel, pp. 158-200.

There is a general tendency to employ cylindrical specimens for testing mechanical properties of Induction hardened steel. The process of hardening was conducted in a cylindrical inductor and sprayer (Fig. 128, p.163). The inside diam. and height of this inductor were 23 and 8 mm. respectively.

Steels 40 and 40 x (chem. anal. see page 120) were investigated. At first, the hardened through specimens were considered. Penetration hardness values (Hv) of specimens representing 40X steel are given in fig. 129, p.166. Hv values are plotted on ordinates and distances from the surface in mm. - on abscissas.

Approved For Release 2001/07/31 : CIA-RDP80-00809A000500170204-4

Approved For Release 2001/07/31 : CIA-RDP80-00809A000500170204-4

Curve 1 - Quenching temp. 960°C and rate of heating 270°C per sec.
Curve 2 - Quenching temp. 840°C and rate of heat. 155°C per sec.
It was established that for steel 40X a through hardening of specimens 10 mm. diam. is secured when a quenching temperature of 1000°C and heating rate of 400°C per sec. are used. The bend test results are presented in fig's 130-133 inclus. pp. 167 and 168. On the ordinates are plotted σ_B ultimate strength and σ_p proportional limit in kg/mm
On abscissas in fig's 130 and 132 are plotted quenching temperatures and in fig's 131 and 133 - the rate of heating. Fig's 130 and 131 refer to steel 40 and fig's 132 and 133 to steel 40X.
On the basis of these results, the author believes that for steel 40 at the 155°C per sec. heating rate, the quenched temperature should be not higher than 920°C, whilst for steel 40X the quenching temperature should be around 1000°C with the rate of heating of 175°C per sec.

A study was made also on the effect of the quenching temperature and rate of heating on the torsion test properties (Fig's 134-138, pp. 170 and 171). In these tests the hardened trough specimens were used.

There is another very important factor besides quenching temperature and rate of heating which should be considered in the study of induction hardening i.e. the depth of hardening.
In his determination of the optimum depth of the induction hardening the author conducted bend, torsion and fatigue strength tests where the depth of hardening was expressed as $\frac{F_{3c}}{F_c}$ where F_{3c} is hardened area and F_c area not hardened.

Approved For Release 2001/07/31 : CIA-RDP80-00809A000500170204-4

Approved For Release 2001/07/31 : CIA-RDP80-00809A000500170204-4

The bend and fatigue test specimens (diam 10 mm.) had $\frac{F_{3c}}{F_c}$ ratios as follows: 0.25; 0.5; 1.0; 2.0. The $\frac{F_{3c}}{F_c}$ ratios for the torsion test specimens were: 0.1; 0.25; 0.5; 1.0; 1.5. The hardened zones of the quenched bend test specimens were of the following thicknesses:

F_{3c}/F_c	Thickness of hardened zone, mm.
0.25	0.50
0.50	0.90
1.00	1.50
2.00	2.10

The bend test results for steels 40 and 40x are given in fig's 140 and 141, p.175. The ratios F_{3c}/F_c are plotted on abscissas and bend strength σ_B and proportional limit σ_p - on ordinates.

The author states that his data indicate that the deflection values in the bend tests of the induction hardened specimens were higher as compared with specimens subjected to a conventional method of hardening, i.e. the induction hardening has a favorable effect on the plasticity of steel.

The thickness of the hardened zones of the torsion test specimens (diam. 20 mm) were:

F_{3c}/F_c	Thickness of hardened zone, mm
0.10	0.50
0.25	1.20
0.50	1.80
1.00	3.10
1.50	3.60

The torsion test results obtained with steels 40 and 40x are shown in fig.142, p.176, where the proportional limits in kg/mm^2 are plotted on ordinates and F_{3c}/F_c ratios on abscissas. It is evident that proportional limits values increase until $F_{3c}/F_c = 1$ ratio is reached. With a further increase in this ratio

Approved For Release 2001/07/31 : CIA-RDP80-00809A000500170204-4

Approved For Release 2001/07/31 : CIA-RDP80-00809A000500170204-4

there is a decrease of those values.

The effect of depth of hardening on the fatigue strength of steel 40X is demonstrated in fig.144, p.184, where F_{3c}/F_c are plotted on abscissas and fatigue strength in kg/mm^2 on ordinate. It may be seen that the fatigue strength values increase with the depth of hardening. The author comes to conclusion that, in general, the induction hardening method has favorable effect on the fatigue strength. The impact toughness versus depth of hardening are plotted in fig. 148, p.192, where F_{3c}/F_c are plotted on abscissas and impact toughness in kg/cm^2 on ordinate. a - steel 40 and b - steel 40x. It may be seen that there is a considerable drop in the impact toughness when F_{3c}/F_c changes from 0.25 to 0.5. With a further increase of this ratio the impact toughness values increase somewhat.

The following results were obtained in the comparison tests with the specimens subjected to a conventional method of hardening and the induction hardened specimens:

Steel	Impact toughness kg/cm^2	
	Induction hardening	Conventional method of hardening
40	7.75	2.84
40X	7.07	2.77

Approved For Release 2001/07/31 : CIA-RDP80-00809A000500170204-4

Approved For Release 2001/07/31 : CIA-RDP80-00809A000500170204-4

Part 7 - Induction hardening of Case Hardened Steel pp. 201-238

Steels, types 20 and 20x were investigated.

Steel	C	Mn	Si	Cr	Ni	P	S
	percent						
20	0.21	0.53	0.20	—	—	0.040	0.040
20X	0.23	0.35	0.15	0.85	—	0.042	0.045

The carburizer used consisted of 80% coal and 20% sodium carbonate. The cementation procedure was as follows: Heating to 900° - 920°C, holding for 13.5 hrs. and cooling in air.

The structure of case hardened layer, steel 20, consisted of lamellar pearlite and cementite boundaries (Fig.151, p.205).

Induction hardening was conducted at different quenching temperatures and rates of heating. Quenching temperatures ranged from 760° to 1200°C and rates of heating were 90, 225 and 450°C per sec.

The quenching medium was water at 20°C.

The structures of this hardened layer after quenching are illustrated in fig's 152-159, pp. 207 and 208. Fig.152 - Quench. T. 760°C and rate of induction heat. 90°C per sec.; fig.153 - Quench T. 960°C, rate of heat 450° per sec; fig. 154 - Quench T. 1100°C, rate of heat 450°C per sec.; fig.155 - Quench T. 1200°C, rate of heat 450°C per sec.; fig 156 - Quench T. 880°C, rate of heat. 90°C per sec.; fig.157 - Quench T. 960°C, rate of heat 90°C per sec.; fig.158 - Quench T. 1100°C, rate of heat 90°C. per sec.; fig.159 - Quench T. 1200°C, rate of heat 90°C per sec.

On the basis of his microscopic examinations, the author comes to conclusion that the cementite network dradually disappears with an increase in quenching temperature and the greater is the rate

Approved For Release 2001/07/31 : CIA-RDP80-00809A000500170204-4

Approved For Release 2001/07/31 : CIA-RDP80-00809A000500170204-4

of heating the higher is the temperature at which the network is completely eliminated. As temperature increases, the network becomes thinner and appears broken in some places but there is no agglomeration of the cementite particles.

Similar tests conducted with steel 20x indicate (fig's 160, 161, 162, p.210) that the initial structure of the case hardened layer of this steel contains large carbide particles which are very stable and cannot be eliminated even at very high temperatures.

This structure is considered as undesirable for the induction hardening process.

Fig. 163, p.211 shows the surface hardness Rc versus quenching temperature relation at different heatinh rates for the case hardened steel, type 20x. It may be noticed that the maximum hardness (Rockwell C, 66) was obtained with quenching temp. about 880°C and rate of induction heating V = 450° C per sec.

The transverse hardness values Hv of the case hardened layer of steel 20 for different quench. temp. and rates of induction heating are plotted (ordinates) on fig's 164-166.

Fig.164, p.213, quench. temp. 760° C; fig.165, p.214, temp.840° C; fig. 166, p.215, temp. 960° C. The changes in the transverse hardness at different quenching temperatures are given in fig's 167 and 168, p.216. Fig. 167 - the rate of induction heating was 90° per sec. Fig.168 - this rate was 450°C per sec.

In the static transverse strength (bend) tests the best results were obtained for the case hardened steels 20 and 20x

Approved For Release 2001/07/31 : CIA-RDP80-00809A000500170204-4

Approved For Release 2001/07/31 : CIA-RDP80-00809A000500170204-4

with quench. temp. 960 C and rate of heat. 200°C per sec. (fig's 177 and 178, p.228).

The highest impact toughness values (fig's 179 and 180, pp. 230 and 231) were observed for the case hardened steels 20 and 20x at quench. temp. 960° C and rate of induction heat. 400°C per sec.

The fatigue test results of the case hardened steel 20 are presented in table 13, p.236, where the second column shows the rate of induction heating °C per sec.; The third - quenching temp. °C; the fourth - surface hardness Rc; the fifth - fatigue strength σ_p in kg/mm² (on the basis of 5 millions cycles).

Part 8 - Tempering of Induction Hardened Steel, pp. 239-261

The effect of tempering on structure and mechanical properties of structural steel was studied by K.A.Malisheff and V.A.Pavlov. Chemical analyses of these steels are given in table 14, p. 240. The conclusion was drawn that the maximum effect of tempering on the induction hardened steel is developed at a rate of heating of 150°C per sec.

The effect of tempering on the induction hardened tool steels was investigated by the author (steels 9XC and XВГ, p.120). The martensitic structure extending throughout an entire cross section of specimens was observed at a rate of heating of 50°C per sec. and quench T. 920°C; rate of heat, 100°C per sec., quench T. 960°C, rate of heat 150°C, quench T 1000°C; rate of heat, 200°C, quench T. 1040°C. The cooling medium was water at 25° - 30°C. The tempering temp. ranged from 150° to 500°C. The holding time at those temperatures was 1.5 hrs. The quenched and tempered

Approved For Release 2001/07/31 : CIA-RDP80-00809A000500170204-4

Approved For Release 2001/07/31 : CIA-RDP80-00809A000500170204-4

specimens were subjected to the Charpy impact and Rockwell hardness tests. Results obtained are presented in fig's 189 (steel XBΓ) and 190 (steel 9xC), p.246. Graph.1 - Rate of heat 50°C per sec., quech. T. 920°C; graph.2 - Rate of heat 100°C per sec, quench. T. 960°C; 3 - Rate of heat 150°C per sec., quench T. 1000°C, 4 - 200°C per sec., quench T. 1040°C. Tempering temperatures are plotted on abscissas, Impact values kg/cm^2 and Rc are plotted on ordinates. The graphs not indicated by numbers (fig.189) refer to the impact test values obtained for the same XBΓ steel but hardened by conventional methods. It may be noticed that with an increase of tempering temperature there is a decrease in hardness. The impact values increase at first (until T. 200°C is reached), then they decrease, the lowest values being observed at 300°C.
With a further raise of tempering temperature, there is a steady and considerable increase of impact values.

It is noteworthy that the greater are the rate of an induction heating and quenching temperatures, the higher are the impact values of tempered steels. The author believes that the greater are these factors (rate of heating and quench. temp.) the larger is the amount of residual austenite.

The impact values (kg/cm^2) versus Rockwell hardness Rc for the induction hardened and tempered steel XBΓ are presented in fig. 191, p.250. Graph No.1 Rate of heat. 50°C per sec. and quench. T. 920°C, No.2 - Rate of heat 100°C, quench. T. 960°C; No.3 - Rate of heat. 200°C and quench. T. 1040°C. Graph not

Approved For Release 2001/07/31 : CIA-RDP80-00809A000500170204-4

Approved For Release 2001/07/31 : CIA-RDP80-00809A000500170204-4

numbered refers to the conventionally hardened specimens. It may be seen that for the same impact values the induction hardened and tempered specimens possessed greater hardness as compared with those hardened by a conventional method. Advantages of induction heating for tempering are also discussed.

Part 9 - Induction Normalizing. pp. 262 - 279.

An effect of the rate of induction heating and normalizing temperature was studied by the author on structural steel No.45 (Chem. anal. see p.120).

In fig. 204, p.266 is shown a horizontal inductor for heating cylindrical billets.

Tensile test specimen used in these tests is given in fig. 205, p.267, where a - specimen prepared for induction heating (diam. at the middle 12 mm) and b - specimen machined after heating, d =10 mm).

The rates of induction heating used were 50°, 100°, 150°, 200° and 250° C per sec. The normalizing temperatures ranged from 800° to 1080° C.

The structure of the furnace-normalized specimens is illustrated in fig. 206 p.269 while the structures of specimens normalized by induction heating are presented on fig's 207 - 211, pp.269 and 270.

Fig. 207 Rate of heat 150° C per sec. T. 960° C; Fig. 208 - Rate of heat 150° C, T. 1040°; Fig. 209 - Rate of heat 50° C, T. 880° C; Fig. 210 - Rate of heat 250° C, T. 1000° C; Fig. 211 - Rate of heat 250° C, T. 1080° C.

Approved For Release 2001/07/31 : CIA-RDP80-0

Approved For Release 2001/07/31 : CIA-RDP80-00809A000500170204-4

It was concluded that different rates of induction heating a normalizing temperature higher than 1000°C is undesirable. With a heating rate of 250°C per sec. and normalizing temperature 1080°C all free ferrite forms a network around the grains of pearlite.

On the basis of his metallographic and hardness examination the author believes that in an induction normalizing, the most satisfactory results may be obtained at temperatures somewhat higher than those used in the furnace-normalizing process. The effect of the heating rate and normalizing temperature on the tensile strength test properties is illustrated in fig's 213 (yield point and tensile strenght), 214 (elongation) and 215 (reduction of area), p.273. The rate of heating is plotted on abscissa and normalizing temperature is indicated on curves. The most satisfatory results were obtained with normalizing temperature 920° - 960°C and the rate of heating 150° per sec.

Part 10 - Technologic advantages of the induction hardening process and adoptionability to it in the industrial conditions. pp. 280 - 312. This part does not seem be of interest to the American Metallurgists.

Bibliography, pp. 313-316

There are 81 references, including 7 references to foreign authors.

Approved For Release 2001/07/31 : CIA-RDP80-00809A000500170204-4

Approved For Release 2001/07/31 : CIA-RDP80-00809A000500170204-4

Reviewer's remarks:

In the Reviewer's opinion this book is a valuable contribution to our knowledge on Induction Hardening. It covers thoroughly different problems involved in this process. Most of the conclusions drawn by the author are supported by results of his own extensive investigations. The author demonstrates very well that there are two main factors governing induction hardening processes. These factors are: temperature and heating rate.

It may be noted, however, that many of the photomicrographs are not distinct enough and no details are given as to etching ~~Stiching~~ reagents and magnifications used.

25X1X

[redacted]

July 14, 1953

Approved For Release 2001/07/31 : CIA-RDP80-00809A000500170204-4

[redacted]

METALLURGY OF STEEL. Open Hearth Process. (Metallurgiia Stali Martenovskii Process), K.G. Trubin and G.N. Oyks, Book 703 pages, Government Scientific Technical Publishing House of Ferrous and Non-Ferrous Metallurgy, Moscow, 1951.

This book is divided into 28 parts. It is recommended as a College Text Book.

Introduction pp. 13-26. The historical development of Ferrous Metallurgy in Russia is described. Fig. 1, p.20 showing the progress of production of steel and cast iron is probably of interest. Production is given in thousands of tons: a - steel, b - cast iron.

Part I. General Principles of the open-hearth Production, pp 29-77

Fig. 3, p.45 illustrates the mechanism of oxygen transfer from the gaseous furnace atmosphere to the molten metal by means of slag.
The top zone is gaseous atmosphere, the middle (shaded) zone is slag and the bottom zone is molten metal.
The principal transfering agent is Fe O which is oxydized into Fe_2O_3 and is always present in the open-hearth slag.
It is very probable that oxygen is dissolved in the metal in the form of Fe O and not in its gaseous form.
Therefore the oxydation by gaseous oxygen in the open hearth process takes place only during the melting period.
It also occurs to some extent during the vigorous boiling

Approved For Release 2001/07/31 : CIA-RDP80-00809A000500170204-4

of the melt when drops of liquid metal are thrown through the slag layer into the furnace atmosphere.

Fe O plays a very important role during the refining of the melt. Temperature condition in different locations of the bath, oxygen consumption, oxydation and reduction of iron, silicon, manganese, and phosphorus as well as oxydation of carbon are discussed (pp. 45-74, fig's 5-7 inclus.)

During boiling, the temperature of the bath is fairly uniform The temperature of the slag is 1° to 47° C. higher than that of the molten metal. The tapping temperature depends upon the chemical composition of the metal. For low carbon steel it is usually about 1600° C. The total normal oxygen consumption is 2.5% to 3.5% of the weight of charge.

67% of this amount is consumed for melting and 33% during the boiling period. Studies of the equilibrium of C - O system at different pressures were carried out in different foreign laboratories. A summary of these results is presented in fig. 8, p.75. Carbon percentages are plotted on abscissa and oxygen on ordinate. Mark ● refers to pressure of 1 atm., mark ◒-5 atm., ○ - 10 atm, ⊗ - 20 atm.

It is known that equilibrium condition is characterized by a constancy of the product [%C][%O], i.e.

$[\%C][\%O] = m$, where m 0.0025 at 1560° - 1620°C and with low carbon concentrations.

or $[\%C][\%FeO] = m$, where $m = 0.0112$ at 1600°C

Approved For Release 2001/07/31 : CIA-RDP80-00809A000500170204-4

Approved For Release 2001/07/31 : CIA-RDP80-00809A000500170204-4

Similar experiments were conducted by different Russian investigators under the open-hearth melting conditions. In fig. 9, p.76 one may see the difference between the results obtained under equilibrium (solid line) and actual (shaded area) open-hearth melting conditions.

[%C] [% O] versus %C relation at 1 atm. pressure is presented in fig. 10, p.77, where A - experimental data obtained at equilibrium condition and B - average values obtained under actual open-hearth melting conditions.
It may be seen that product [%C] [%O] is not exactly ~~concultant~~ constant but increases with an increase in the carbon concentration.
It follows, therefore, that no equilibrium of the carbon-oxygen reaction is attained in the open-hearth process and there is usually an excess of dissolved oxygen present in the bath.
The dependence of the value *m* upon the carbon concentration in the bath has ~~to~~ no satisfactory explanation thus far.
The theory advanced by American authors on the change of the oxygen's activity coefficient as a function of the carbon concentration does not yet have sufficient proof.

~~PART 2~~ -

PART 2 - MATERIALS USED IN THE OPEN-HEARTH PRODUCTION, pp. 78 - 102

Different refractory and insulating materials, fluxes, ferro-alloys, pig irons, iron and steel scrap are described.

Approved For Release 2001/07/31 : CIA-RDP80-00809A000500170204-4

Approved For Release 2001/07/31 : CIA-RDP80-00809A000500170204-4

PART 3 - TYPES AND PROPERTIES OF FUEL, pp. 103 - 109

Common knowledge.

PART 4 - OPEN-HEARTH SLAGS, pp. 111 - 131

Great progress has been made during recent years in the study of the mineralogy of the open-hearth slags. It was shown that they consists of numerous different chemical compounds. The most important compounds (silicates, phosphates, aluminates, ferrites) are tabulated at the bottom of page 115. Acid, basic and amphoteric slag components are given in table 25, p.111. Constituent diagram of system SiO_2 - FeO - MnO is presented in fig. 18; for system FeO - CaO - SiO_2 - fig.19, p.113 and for system $2CaO.SiO_2 - 2FeO.SiO_2$ (a portion of diagram $FeO - CaO - SiO_2$) fig 20, p.114.

For fluidity testing of slags, the straight flow channel apparatus is usually employed. For testing acid slags the diameter of the flow channel was increased by A.D.Kramarov to 9 mm.

According to the authors the spiral type of fluidity apparatus developed by V.G.Grousin and K.N.Ivanov, shown in fig. 25, p.121 is superior to the Herty's apparatus. For fluidity measurement this apparatus is placed into the furnace through the charging door. The relation between fluidity and basic property $\left(\frac{\% CaO}{\% SiO_2 + \% P_2O_5}\right)$ of slag is demonstrated in fig.26, p.122. The slag's fluidity decreases with an increase of it's basic property.

Approved For Release 2001/07/31 : CIA-RDP80-00809A000500170204-4

Approved For Release 2001/07/31 : CIA-RDP80-00809A000500170204-4

PART 5 - DEPHOSPHORIZATION. pp 132 - 150

The constitutional diagram Fe-P cannot ~~yet~~ be considered as well established. In studying different phenomena which take place in the molten bath it is usually considered that phosphorus is present in the form of Fe_3P (15.6% P) or as elementary P.

The method of phosphorus removal from the melt consists of

1. oxydation according to reactions:

$$2[P] + 5[FeO] \rightleftarrows (P_2O_5) + 5[Fe] \quad \text{or}$$

$$2[Fe_3P] + 5[FeO] \rightleftarrows (P_2O_5) + 11[Fe].$$

and 2. formation in the slag of a chemically stable compound with P_2O_5 in order to avoid the reverse reaction. Free P_2O_5 cannot exist in slag for it is unstable at high temperatures. It is now well established that the principal role in dephosphorization is played by CaO, providing that in the slag CaO is in proper proportion with Fe O.

The index of dephosphorization is expressed by some authors as

$$F = \frac{1}{P} \cdot \frac{P_2O_5}{P_2O_5 + FeO}$$

The experimental data show that there is a straight - line relation between this index and Ca O concentration in slag. see fig. 42, p. 143.

The present authors believe that no definite conclusions can be drawn so far from numerous investigations conducted by different workers.

Approved For Release 2001/07/31 : CIA-RDP80-00809A000500170204-4

PART 6 - DESULPHURIZATION, pp 151 - 164

Sulphur is dissolved in iron in the form of Fe S, the melting point of which is 1193°C. In slag, sulphur may be present in the form of various sulphides Fe S, Mn S, Ca S Na_2S, Mg S, Si S, Si S_2, Al_2S_3 Ni S, Co S, WS, Mo S_2 etc. The most important are Fe S, Mn S and Ca S.

In the process of desulphurization, the sulphides' solubility is an important factor. In acid slags this solubility is very small, whilst in basic slags it increases with an increase of the basic property of slag.

Considerable desulphurization takes place in the open-hearth process when there is present 2% Mn or more. It is considered that the desulphurization mechanism in the open hearth melts consist of (1) diffusion of sulphides from the metal to slag

$$[FeS] \rightarrow (FeS)$$

and (2) reaction in the slag-zone when CaO is present:

$$FeS + CaO \rightleftarrows CaS + FeO$$

$$FeS + MnO \rightleftarrows MnS + FeO$$

Homogeneous reactions advance in the slag with great speed, whereas diffusion proceeds at a slower rate. A decisive factor of desulphurization is the basic property of slag, an excess of free Ca O being favorable for homogeneous reaction

$$FeS + CaO \rightarrow CaS + FeO$$

The constant of this reaction is

$$K = \frac{(FeS)(CaO)}{(CaS)(FeO)} \quad \text{or} \quad FeS = \frac{K(CaS)(FeO)}{CaO}$$

Approved For Release 2001/07/31 : CIA-RDP80-00809A000500170204-4

PART 6 - DESULPHURIZATION, pp 151 - 164

Sulphur is dissolved in iron in the form of Fe S, the melting point of which is 1193°C. In slag, sulphur may be present in the form of various sulphides Fe S, Mn S, Ca S Na_2S, Mg S, Si S, Si S_2, Al_2S_3 Ni S, Co S, WS, Mo S_2 etc. The most importent are Fe S, Mn S and Ca S.

In the process of desulphurization, the sulphides' solubility is an important factor. In acid slags this solubility is very small, whilst in basic slags it increases with an increase of the basic property of slag.

Considerable desulphurization takes place in the open-hearth process when there is present 2% Mn or more. It is considered that the desulphurization mechanism in the open hearth melts consist of (1) diffusion of sulphides from the metal to slag

$$[FeS] \rightarrow (FeS)$$

and (2) reaction in the slag-zone when CaO is present:

$$FeS + CaO \rightleftharpoons CaS + FeO$$

$$FeS + MnO \rightleftharpoons MnS + FeO$$

Homogeneous reactions advance in the slag with great speed, whereas diffusion proceeds at a slower rate. A decisive factor of desulphurization is the basic property of slag, an excess of free Ca O being favorable for homogeneous reaction

$$FeS + CaO \rightarrow CaS + FeO$$

The constant of this reaction is

$$K = \frac{(FeS)(CaO)}{(CaS)(FeO)} \text{ or } FeS = \frac{K(CaS)(FeO)}{CaO}$$

Approved For Release 2001/07/31 : CIA-RDP80-00809A000500170204-4

Approved For Release 2001/07/31 : CIA-RDP80-00809A000500170204-4

The complete transformation of soluble in the metal Fe S into practically insoluble CaS, i.e. an approach of concentration (Fe S) to zero requires the maximum concentration in the slag of Ca O and minimum of Fe O.

This consideration explains the fact that a high degree of desulphurization is easily obtained in the blast and electric furnaces.

$FeS + CaO + C = Fe + CO + CaS$ (Blast furnace).

$FeS + CaC_2 + 2FeO = CaS + 3Fe + 2CO$ (Electric furnace).

PART 7 - VARIANTS IN THE PRACTICE OF THE BASIC OPEN-HEARTH PROCESS

pp 165 - 224

The most important variants are the scrap and scrap-ore processes. In scrap process, the charge may consist of steel scrap, of steel scrap and solid pig iron or steel scrap and liquid iron. It is now considered that it is feasible to use a charge made of steel scrap only. The carbon is added in form of graphite, coal, coke, wood etc.

Since steel scrap is not readily fusible it requires a longer time to melt. However the melting period may be shortened by an introduction into furnace of gaseous oxygen.

Other variants of the scrap process, i.e. scrap-solid pig iron as well as scrap-liquid iron are also described at length.

In the scrap-ore process the charge is made of ore, scrap and molten iron. For example, at one of the Russian plants (Kousnetskii plant) the charge was made into their 300 tons open-hearth furnace in the following order:

1 - ore; 2 - limestone; 3 - ore, balance; 4 - scrap, small pieces; 5 - scrap, large pieces; 6 - molten iron.

Approved For Release 2001/07/31 : CIA-RDP80-00809A000500170204-4

Approved For Release 2001/07/31 : CIA-RDP80-00809A000500170204-4

The molten iron is added after the solid portion of the charge is well preheated for $1\frac{1}{2}$ to 2 hrs.

It is necessary to have strict control of slag during melting. An example of the chemical composition of slag in two Russian plants (A and B) is given in table 42, p.201. The figures shown in the first line for plant A refer to the slag taken during the first period of melting, whilst those in the second line relate to the final period.

The basic property of such slag is approximately determined as

$$\frac{CaO}{SiO_2} = 0.8 - 1.4$$

PART 8 - ACID OPEN-HEARTH PROCESS pp. 225-252

In the acid process, the bottom of an open-hearth furnace is made of the refractory materials possessing acid properties. For example, the following method was adopted in one russian plant: the bottom of their furnace is made of silica bricks (dinas, covered by a layer of quartz (97.42% SiO_2; 0.22% Fe_2O_3; 1.24% Al_2O_3; 0.08% CaO; 0.14% MgO), pure quartz river sand (not less than 95 - 96% SiO_2) and also crushed slag taken from acid open-hearth furnace.

There are two variants of the acid process:
1. Silicon reducing or passive and 2. of limited silicon reduction, or active processes.

There are two conditions at which the reduction of silicon takes place: 1. High temperature and 2. presence of weakly acid slag.

Approved For Release 2001/07/31 : CIA-RDP80-00809A000500170204-4

Approved For Release 2001/07/31 : CIA-RDP80-00809A000500170204-4

The fluidity — SiO_2 concentration relation for acid slags is demonstrated in fig. 61, p.233. Line I represents data obtained during the first three hours since beginning of boiling and line II refers to the second period of boiling. In both cases, the slags fluidity increases with a decrease of SiO_2 concentration.

It is well established now that gases dissolved in metals produce a great effect on their properties. The effect of hydrogen dissolved in steel is of particular importance. Slag should play a very important role in the process of gas saturation in steel. This problem is still not fully investigated. In this connection, the data obtained by Yavoyiskiy are of interest. According to him, the amount of hydrogen dissolved in slag (in the acid open-hearth process) depends upon ratio MnO : FeO (in the slag). Fig.64, p.241 presents Yavoyskiy's data on the amount of hydrogen in the bath (medium carbon steel) in the silicon reduction process as related to the ratio $\frac{MnO}{FeO}$ in the slag. Mark ∅ refers to the test samples taken before deoxidation and ○ after deoxidation.

PART 9 - DEOXIDATION, pp. 253 - 285

As it may be seen in the Fe-O constitutional diagram, oxygen is soluble in the liquid as well as in solid iron. Oxygen solubility in molten iron is shown in fig. 71, p.254. It increases with an increase of temperature. It is most probable

Approved For Release 2001/07/31 : CIA-RDP80-00809A000500170204-4

Approved For Release 2001/07/31 : CIA-RDP80-00809A000500170204-4

that oxygen dissolves in the liquid iron in the form of Fe O. There are three methods of deoxydation: 1. Residue method, 2. Diffusion method, and 3. Deoxydation by synthetic slags.

In the residue process oxygen is removed from the liquid steel in the form of oxides of the element used for deoxydation. These oxides float into the slag zone. In general, the process may be expressed by the following reaction:

$$[FeO] + [Me] \rightleftarrows [MeO] + [Fe]$$

$$\text{and } [MeO] \rightleftarrows (MeO)$$

The direction of the above reactions should be to the right. Me designates an element used as the deoxydation agent. The equilibrium constant of this reaction is

$$K = \frac{[FeO][Me]}{[Fe][MeO]} \text{ and}$$

$$[FeO] = K\frac{[Fe][MeO]}{[Me]}$$

It is obvious that the larger the concentration of (Me), the smaller will be the amount of $[FeO]$ remaining in the metal.

Deoxidation by manganese, silicon, aluminum, titanium, zirconium and boron are described. The most potent deoxidiser is aluminum. According to thermodynamics the deoxidation ability of boron

Approved For Release 2001/07/31 : CIA-RDP80-00809A000500170204-4

Approved For Release 2001/07/31 : CIA-RDP80-00809A000500170204-4

is higher than that of silicon, vanadium and titanium.

In practice, the complex deoxidizers are widely used. The most common complex deoxidizers are silicon-manganese and aluminum-manganese-silicon alloys.

Diffusion method. Fe O is soluble in the metal and slag. A decrease of Fe O concentration in slag promotes its diffusion from metal to slag until equilibrium condition, for a given temperature, is established

$$L_{FeO} = \frac{[Fe\,O]}{(Fe\,O)} = const.$$

In general, the process of diffusion deoxidation may be expressed as follows:

$$[Fe\,O] \rightleftarrows (Fe\,O) \text{ and } (Fe\,O) + [Me] \rightleftarrows (Me\,O) + [Fe]$$

In practice, the reduction of iron oxides in the slag is accomplished by an addition of deoxidizing mixtures (powders) containing charcoal, coke or graphite and ferrosilicon.

Deoxidation by synthetic slags. Many attempts were made to deoxidize steel by synthetic slags. The constitutional diagrams of various oxides systems were studied and after many years of research work the excellent results were obtained. The formulas of synthetic slags which can be used for deoxidation and dephosphorization were developed. The following slag composition is recommended for deoxidation:

60% SiO_2; 15% Al_2O_3; 10% CaO; 4% MnO; 10% Na_2O.

or 70% SiO_2; 25% Na_2O; 5% CaO.

Approved For Release 2001/07/31 : CIA-RDP80-00809A000500170204-4

Approved For Release 2001/07/31 : CIA-RDP80-00809A000500170204-4

To secure the maximum metal-slag contact area, the metal is poured from a great height (up to 6 met.) and with a great velocity into the ladle containing the synthetic slag. It is of particular importance to have slags containing a very small amount of Σ(Fe O + Mn O). An example of such slag is given as follows: 65% CaO; 13% SiO_2; 2% Al_2O_3; 15% CaF_2; 4% MgO; < 1% FeO; 0.20% MnO; 0.10% P_2O_5 and up to 1% CaC_2.

PART 10 - ALLOYING AND ALLOY ELEMENTS pp. 286 - 300

In table 66, p. 286 different elements are arranged according their solubility in pure iron at the temperatures employed in the steel melting processes. In the first column of this table are metals which are completely soluble in the liquid iron. In the second column are those which are partly soluble. In the third columns - metals, practically insoluble. In the fourth column are partly soluble non-metallic elements, and in the fifth column are metallic elements which are in the gaseous state at the steel melting temperatures. Their solubility is unknown. Not all of the elements listed in the table find their application in steel production. On other hand, some elements, like Zr, Nb and B, were not included because no complete date on their behavior in solution are available. Thermodynamic relation between activity of various elements in solution and their free energy is discussed.

Approved For Release 2001/07/31 : CIA-RDP80-00809A000500170204-4

Approved For Release 2001/07/31 : CIA-RDP80-00809A000500170204-4

PART 11 - DEOXIDATION BY THE RESIDUE METHOD AND ALLOYING. THE CONDITION OF BATH AT THE MOMENT OF DEOXIDATION. pp 301-306

This part is of no particular interest.

PART 12 - REFINEMENT OF HIGH PHOSPHORUS IRONS pp 307-315

Refinement of irons containing 0.3 to 1.4%P is considered unprofitable. It becomes profitable only with higher P concentrations on account of the by-product formed, i.e. slag containing more than 14% P_2O_5. The process is usually divided into two periods and is conducted in two open-hearth furnaces. In the first period a necessary amount of ore and limestone is added to the solid or liquid charge of the high-phosphorous iron and phosphorus rich slag is collected. The melt produced in this furnace contains approximately 1.7% C, 0.2% Mn, 0.2 - 0.3%P and traces of silicon. The final refinement is then carried out in the second furnace. At first, ore and limeston are charged into this furnace and heated until they are fused. Next, the molten steel is poured there from the first furnace. The whole procedure is schematically illustrated in fig. 86, p.309. On this sketch are whown two furnaces which may be used in the first period of the process and one furnace used for the final refinement (second period). It was found however too difficult to synchronize the work in two furnaces (1st and 2nd period furnaces) and in practice the process was modified. Four variants of the process are described.

Approved For Release 2001/07/31 : CIA-RDP80-00809A000500170204-4

Approved For Release 2001/07/31 : CIA-RDP80-00809A000500170204-4

PART 13 - CHROMIUM REMOVAL FROM THE CHROMIUM CONTAINING CHARGES.

In the open-hearth chromium removal process, chromium is oxidized and the oxides are removed with the slag during the first period of melting.

Properties of the basic chromium-bearing slags, conditions of chromium reduction from slags are described.

A silicon content of greater than 0.2% Si in the metal strongly resists transfer of the chromium into the slag. This is illustrated in fig. 99, p.326, where the distribution coefficients $\frac{(Cr)}{[Cr]}$ are plotted as ordinates and silicon Wt. percents in the melt [Si] along the abscissas.

A similar relationship is observed for manganese. Fig. 101, p. 327 shows $\frac{(Cr)}{[Cr]}$ vs. % Mn (in the metal) relation for different manganese contents in the slag (Mn). Distribution coefficients $\frac{(Cr)}{[Cr]}$ are plotted on ordinates and manganese percents in molten metal on abscissas. The top figures indicate the manganese content in the slag.

PART 14 - PRODUCTION OF HIGH-TEST AND SPECIAL STEELS, pp. 353-364

Production of nickel-chromium, chromium-molybdenum, high-manganese (14% Mn) and automotive steels are discussed. In table 64, p.362 the approximate compositions of automotive steels used in different countries are given. In the first column, names of countries are listed in the following order: U.S.S.R. England and Germany.

Approved For Release 2001/07/31 : CIA-RDP80-00809A000500170204-4

Approved For Release 2001/07/31 : CIA-RDP80-00809A000500170204-4

PART 15 - COMBINATION STEEL MELTING PROCESSES, pp.365-390

The following duplex processes are briefly described: Bessemer acid - basic open hearth, Thomas - basic open hearth, active mixer, basic - acid open hearth and cupola - open hearth processes.

The construction of an active mixer (refiner) is that of a rocking large open hearth furnace. Its capacity is 200 to 500 tons and the depth of bath is 1 to 2 meters.

PART 16 - CASTING OF STEEL, pp. 393-461

Different details related to casting of steel are illustrated in fig's 111-138.

Steel ingot molds are usually made of cast iron, but sometimes they are made of steel. The average life of cast iron molds is 60 to 100 heats for regular steel and still less for high test steels. The most suitable material for ingot molds is cast iron, the structure of which consists of a pearlitic-ferritic matrix and a small amount of fine graphite.
The presence of free carbide is not permissible. For small molds iron containing 10 to 15% ferrite is recommended and for large molds 20 -60% ferrite.
The following composition was recommended by N.N.Blinoff:
C, 3.3 - 4.0%; Si, 1.0 - 2.2%; Mn, 0.8 - 1.0%; P, 0.1 - 0.25%; S < 0.1%

Approved For Release 2001/07/31 : CIA-RDP80-00809A000500170204-4

Approved For Release 2001/07/31 : CIA-RDP80-00809A000500170204-4

It is also recommended that cast iron be melted in a cupola. Molds of a higher durability may be produced of cast iron to which 0.5% Cr, a small amount (0.2%) of titanium and molybdenum are added. Addition of chromium increases stability of iron carbides during heating and prevents the cast iron growth at 500° - 600° C. Nickel addition increases the resistance to growth.

Different types of ingot-molds are shown in fig's 139 and 140, pp. 441 and 443.

PART 17 - POURING PRACTICE , pp 462 - 472

This part is of no particular interest.

PART 18 - PIPE FORMATION AND AXIAL UNSOUNDNESS PREVENTION METHODS pp. 473 - 489

The principal methods to prevent unsoundness in steel ingots are mechanical and thermal methods. Mechanical arrangement of compression is illustrated on the sketch, fig. 149 p.474. Ingot mold W filled with liquid steel is brought on carriage K under press rest C. Compressing load is 15 atm. Heavy ingots (53 and 133 tons) were compressed for 2-3 hours. The reduction in height reached 11%. Fig. 150, p.474 shows the longitudinal cross-section of compressed steel and the shrinkage cavity. According to the authors this method may produce excellent results in those castings the central portion of which has to be drilled out.

Approved For Release 2001/07/31 : CIA-RDP80-00809A000500170204-4

Approved For Release 2001/07/31 : CIA-RDP80-00809A000500170204-4

Fig. 152 p.475 shows the compression of liquid steel by gas. This method was found to be unsatisfactory.

In fig. 157, p.479 is presented the method developed by V.V.Lermontoff. Mold with liquid steel is jolted by means of a lever (5-8 times per min., drop 10-12 mm) during cooling. This method proved to be satisfactory. The vertical cross section of a steel ingot produced by this method indicates the absence of gas cavities.

Different methods of heating the top part of ingot to keep it hot during feeding are also discussed.

PART 19 - TEMPERATURE AND SPEED OF THE CASTING PROCEDURE, pp 490-495

Tapping temperature of steel, alloy steel in particular, should be 120°-130° C above the Liquidus. Temperature measurements should be made with Pt/Pt.Rh thermocouple. Holding time of steel in the ladle should be 5 - 15 min. The pouring rate shouldn't be higher than 2.5 tons per min.
Pouring time VS. Ingot's weight relation is presented diagrammatically in fig. 163, p.494. The ingot's weight is plotted as abscissa and pouring time as ordinate.

PART 20 - CRYSTALLIZATION OF STEEL POURED INTO MOLD, pp.496-527

The liquid state was considered as analogous to the gaseous state, characterized by the term "a molecular chaos"
Some recent investigators remark that although the molecules (atoms) in the liquid, as we have in the gas, are all the time

Approved For Release 2001/07/31 : CIA-RDP80-00809A000500170204-4

Approved For Release 2001/07/31 : CIA-RDP80-00809A000500170204-4

in motion, the intermolecular distances in a liquid remain constant. A hypothesis was advanced by some that in the liquid metal, particularly at temperatures close to the liquidus, are present very fine groups of microparticles the structure of which is similar to that of the solid metal. The authors state, however, that there are not enough data as yet to draw any definite conclusion. Different factors which affect crystallization of steel are discussed. These factors are: temperature of mold and liquid steel, wall thickness of mold, the rate of pouring and motion of liquid metal in the mold, material and specific heat of the mold, chemical composition of metal, gases and mass effect of cast ingot. Tscernoff's sketches of dendrites (fig.166 and 167, p.505) and macrostructure (fig. 169, p.509) showing three zones of crystallization are presented. A portion of the iron-carbon constitutional diagram showing three zones of crystallization is given in fig.173, p.526. I - Zone of primary crystallization, II - Zone of granulation, and III - Zone of secondary crystallization.

PART 21 - INGOT'S STRUCTURE OF KILLED (quiet) STEEL, pp. 528-549

A schematic drawing of the crystalline structure of a steel ingot is presented in fig. 175, p.529. An attempt was made by Troubin to establish a relation between the pipe cavity's formation in a steel ingot and the gas saturation in the metal. Specific gravities of steel and gas solubility values (at 1 atm. pressure) in iron for different temperatures are shown in fig.'s 177 and

Approved For Release 2001/07/31 : CIA-RDP80-00809A000500170204-4

Approved For Release 2001/07/31 : CIA-RDP80-00809A000500170204-4

178, p.552, respectively. It is to be noticed that within the solidification interval these is a pronounced decrease of gas solubility and an increase of specific gravity.

The pipe cavity is filled up with gases, mostly hydrogen. The gas pressure developed may be as high as 3 atm.
The chemical analysis of those gase was found to be: 92.9% H_2; 1.5% CO; 1.2% CH_4; 1.4% CO_2; 1.5% O_2; 1.5% N_2.

Some investigators claim that HCN may also be present.

According to V.M.Tagueev, the time of complete solidification of a cast ingot may be calculated as follows:

$$t_K = 0.112 R^2$$ where

t_K is time of complete solidification in minutes and R - radius in cm. (for square and polyhedral ingots, radius of inscribed circumference).

PART 22 - INGOT'S STRUCTURE OF WILD STEEL, pp 550 - 566.

Ingot's structures of wild steel are illustrated in fig.185, p.552. The structure is not uniform.

According to D.K.Tchernoff (1876) the largest portion of gases are evolved at the very beginning of solidification of steel and they consist mostly of CO whereas according to Müller (1879) the main factor responsible for blow holes is hydrogen.
The scheme of blowhole formation, as described by Tchernoff in 1876, is illustrated in fig.186, p.554. According to him, the form

Approved For Release 2001/07/31 : CIA-RDP80-00809A000500170204-4

Approved For Release 2001/07/31 : CIA-RDP80-00809A000500170204-4

of a blowhole may change in accordance with the relative rates of the blow hole's formation and steel crystallization. This is illustrated in fig.187, p.555.

PART 23 - SEGREGARION IN STEEL INGOTS, pp 567 - 605

An example of chemical heterogeneity is presented in table 108 p.573. This table is a summary of the chemical analysis results of 17 ingots, each weighing 1.8 tons and cast of a killed steel into similar molds. The samples were taken from 8 different spots of each ingot (see fig. 195, p.574). Segregations of V and Λ types are discussed and illustrated in fig. 196, p.574 and fig.197, p.575. Fig. 196 shows macrostructure (deep etching) of a heavy ingot and fig. 197 - sulphur prints of a 3 tons ingot. Fig. 198, p.576 illustrates macrostructure of an ingot weighing 28 tons and cast into a sand mold. Sulphur prints of a wild steel ingot are shown in fig.200, p.587. Different factors affecting segregation are considered.

PART 24 - GASES IN STEEL, pp 606-653

Gases can diffuse only in the atomic state. The rate of gas diffusion increases with an increase of it's partial pressure. The solubility of atomic gas in the metal VS. temperature is expressed by formula $S = C e^{\frac{E_s}{2KT}}$ where S - solubility of gas in metal; C - constant; E - heat of solution, or heat of formation of a chemical compound; K - Bolzman's constant; T - absolute temperature.

Approved For Release 2001/07/31 : CIA-RDP80-00809A000500170204-4

Approved For Release 2001/07/31 : CIA-RDP80-00809A000500170204-4

A comprehensive study of gases evolved during crystallization of steel ingot was made by I.I.Soubbotin. The data obtained are presented in table 120, p.630. In the first column of this table are given samples' numbers, in the second-minutes, in the 3rd to 7th columns - percents of O_2, CO, H_2, CO_2 and N_2.

PART 25 - NON-METALLIC INCLUSIONS IN STEEL. pp. 654 - 676.

Endogenous and exogenous types of inclusions are described. Ternary diagrams of different oxides systems are presented in fig's 227, p.657 to 231, p.661 inclusive.

PART 26 - QUALITY CONTROL OF STEEL INGOT AND EVALUATION OF PROPERTY OF STEEL. pp.677-683

This part is of no particular interest to American metallurgists

PART 27 - SAFETY MEASURES USED IN THE OPEN-HEARTH FOUNDRY. pp.684-695

Ditto.

PART 28 - CALCULATIONS OF MATERIAL AND THERMAL BALANCES IN THE OPEN-HEARTH PROCESS. pp. 696-758

Ditto.

Approved For Release 2001/07/31 : CIA-RDP80-00809A000500170204-4

Approved For Release 2001/07/31 : CIA-RDP80-00809A000500170204-4

BIBLIOGRAPHY, pp. 759-763

There are 195 references, 54 of which are foreign publications. Unfortunately, titles of foreign publications are written in Russian letters.

Reviewer's remarks

Some paragraphs of the book are too sketchy and not clear enough, whereas other are unduly lengthy and contain too many unnecessary details, theoretical discussions and repetitions. In general, the material presented in this text book is fairly well known to American Metallurgists. Nevertheless some parts of the book selected by the reviewer would probably be of some interest. It is very significant that, evidently for political reasons, in their discussion on crystallization of steel no mention was made by the authors of the work of Colonel N.T.Belaiew, the ablest pupil of prof. Tchernoff. In refering to his work Sauveur ("The Metallography and Heat Treatment of Iron and Steel", Albert Sauveur, Second Edition 1916, p.206) stated that "we are indebted to Colonel Belaiew more than to any one else for our knowledge of the crystallization of steel".

25X1X

[redacted]

April 17, 1953

Approved For Release 2001/07/31 : CIA-RDP80-00809A000500170204-4

Approved For Release 2001/07/31 : CIA-RDP80-00809A000500170204-4

BIBLIOGRAPHY, pp. 759-763

There are 195 references, 54 of which are foreign publications. Unfortunately, titles of foreign publications are written in Russian letters.

Reviewer's remarks

Some paragraphs of the book are too sketchy and not clear enough, whereas other are unduly lengthy and contain too many unnecessary details, theoretical discussions and repetitions. In general, the material presented in this text book is fairly well known to American Metallurgists. Nevertheless some parts of the book selected by the reviewer would probably be of some interest. It is very significant that, evidently for political reasons, in their discussion on crystallization of steel no mention was made by the authors of the work of Colonel N.T.Belaiew, the ablest pupil of prof. Tchernoff. In refering to this work Sauveur ("The Metallography and Heat Treatment of Iron and Steel", Albert Sauveur, Second Edition 1916, p.208) stated that "we are indebted to Colonel Belaiew more than to any one else for our knowledge of the crystallization of steel".

25X1X

[redacted]

April 17, 1953

Approved For Release 2001/07/31 : CIA-RDP80-00809A000500170204-4

Approved For Release 2001/07/31 : CIA-RDP80-00809A000500170204-4

25X1A

[redacted]

doc ct

IRON ALLOYS - Vol I

Iron-Chromium-Alluminum Alloys by I. I. Kornilov of the Institute of General and Inorganic Chemistry, Laboratory of the Iron Alloys. Published by Academy of Science, Moscow 1945.

Part 1 of this book consists of the general theory of equilibrium diagrams.

Part 2 is a discussion of binary equilibrium diagrams of Fe-Cr, Fe-al, and Cr-Al.

Part 3 is a discussion of the ternary equilibrium diagram of Fe-Cr-Al.

Part 4 is a microscopic study of the various phases that appear in the Fe-Cr-Al teruary diagram in the annealed and heat treated conditions.

Part 5 is a discussion of the physical properties of the teruary solid solution.

The electrical resistance of annealed Fe-Cr, Fe-Al and Cr-Al binary alloys were found to vary as follows:

(1) In Fe-Cr alloys, it was found that as the Cr in Fe increased the electrical resistance increased. The percentage of Cr varied from 0 to 45.05.

(2) The Fe-Al alloys showed that as the Al increased in the Fe, the electrical resistance increased up to about 23.6% Al; then the resistance dropped and again began to rise; but it did not increase to the extent reached with 23.6% Al. The maximum Al recorded is 38.9%.

(3) The Cr-Al alloys showed that as the Al increased in the Cr the resistance increased and reached a maximum at 14.08% Al and then dropped. The resistance again began to rise and this was followed by another drop. The maximum Al recorded was 21.65%.

Approved For Release 2001/07/31 : CIA-RDP80-00809A000500170204-4

In each case the pure metals showed the lowest resistance. Results show that either Al or Cr or both when added to Fe increases the electrical resistance.

The results of the heat treated samples were similar to the annealed ones.

The same general results were obtained in thermal expansion, namely, the greater the amounts of addition elements added to iron, the greater the thermal expansion between 0 and 1000°C.

The parameter's values A for the binary Fe Cr and Fe Al alloys are taken from the foreign literature (Preston; A. J. Bradley and A. Jay) data. The parameter's values for ternary Fe-Cr-Al alloys are V. G. Kousnetsoff's unpublished data. The first column of the table shows atomic percents, the 3rd, 5th, 7th and 9th -- weight percent. Within the limits of ternary solid solution α_3 a trend in parameter change is similar to that of binary Fe-Al alloys. It may be supposed, therefore, that in the Fe-Cr-Al system, in alloys adjacent to Fe-Al side there is also a formation of the superstructure of the type of Fe_3 Al and Fe Al compounds. Steinberg's magnetometer was employed for the study of the magnetic properties of the ternary solid solution. The Curie points were determined when heating speciments in the magnetometer. The intensity of the magnetic force was measured by means of a galvanometer. The ternary alloys, whose magnetic properties were studied by the author, included alloys containing up to 100% of chromium and up to 25% aluminum. The change in magnetic properties with temperature of some alloys is shown. The compositions of these alloys are indicated on the curves as Cr %/Al% ratios.

Part 6 is a discussion of the mechanical properties of the Fe-Cr-Al teruary solid solutions.

Approved For Release 2001/07/31 : CIA-RDP80-00809A000500170204-4

Approved For Release 2001/07/31 : CIA-RDP80-00809A000500170204-4

Here like in the electrical resistance and thermal expansion results, the hardness increases as the amounts of Al and Cr are increased in the iron.

Tensile strengths and percent elongations are shown below.

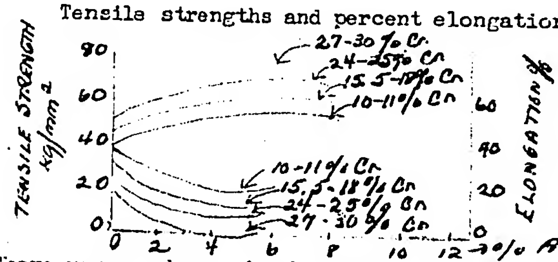

It will be noted that the maximum tensile strength was obtained from the Fe alloy containing 30% Cr and 10% Al.

There was no change in the impact toughness of iron with the addition of chromium up to 15-16%. As the chromium is increased above 16% there is an abrupt decrease in the impact properties. An abrupt decrease in impact properties also occurs with more than 4% aluminum.

Part 7 shows the results of oxidazation tests due to heat.

The results of these tests showed that with the increase of Cr up to 17%, the oxidization decreased, and above this amount the effect of Cr was less than the effect of Al. With 10% Al the good results were obtained. However, the Cr added materially to the oxidization resistance of the alloy. With 65% Cr and 10% Al the best results were obtained. The tests were run at temperatures up to 1400°C and for 120 hours.

Part 8 shows the influence of a fourth component on the properties of the ternary solid solution.

The heat resistance of the Fe-Cr-Al alloy decreases with the increase in carbon content. The presence of titanium within the limits of its solubility in the solid solution has a beneficial effect on the heat resistance.

Approved For Release 2001/07/31 : CIA-RDP80-00809A000500170204-4

Approved For Release 2001/07/31 : CIA-RDP80-00809A000500170204-4

Part 9 gives the production technology of Cr-Al stuls.

The author refers to W. Hessenbruch's work (Metalle and Legierungen fur hoke Temperaturen, Springer, Berlin, 1940).

Part 10 gives the methods used to obtain carbon free Fe-Cr-Al alloys.

Part 11 gives the technology of production of heat resisting Fe-Cr-Al alloys.

The raw materials employed for the preparation of these alloys were: 1. Armco Iron 2. Chromium-aluminum hardeners and ferro-chromium-aluminum hardeners. 3. Ferro-aluminum (up to 54.5% Al). 4. Aluminum powder. Slag used corresponded to the ternary eutectic whose melting point is 1345°C.

Melting was carried out in high frequency induction furnaces of laboratory or production types.

Method 1 - Armco iron is charged and melted under a layer of slag and all necessary additions are then made. Method 2 - Armco iron and pieces of hardener are melted under slag and the remaining portion of charge is added. The effect of vanadium, molybdenum, zirconium, niobium (columbium) and titanium on crystallization of ingots was studied. These elements were added in the form of their ferro-alloys 5 minutes before pouring. The metal was poured at 1550°-1560°C. Cast ingots were longitudinally sliced in halves and their macrostructures were examined. It is shown that high additions of Molybdenum, zirconium and niobium (a, 0.49% Mo; b, 0.47% Zr and V, 0.46% Nb) failed to produce a significant effect on the primary structure of ternary solid solution α_3. The somewhat better results were obtained with 0.3% and 0.5% additions of vanadium. The most beneficial effect on the refinement of the primary

Approved For Release 2001/07/31 : CIA-RDP80-00809A000500170204-4

Approved For Release 2001/07/31 : CIA-RDP80-00809A000500170204-4

structure of ternary solid solution α_3 was obtained with additions of titanium. The ingots free from titanium show a large zone of trans-crystallization and concentric cracks, whereas those containing 0.4% Ti possess a fine crystalline structure.

Ternary alloys, containing 30% and up Cr, located within zone $\alpha_3 + 5$ phases, cannot be cold drawn. The alloys situated within a zone of ternary solid solution α_3 containing chromium up to 27-28% and aluminum up to 6-7% can be drawn. The absence of carbon and a reduced content of silicon make the structure of alloys homogeneous and permit an increase in the limit of the aluminum content. The same factors permitted the production of wire of 0.03 - 0.04 mm. diam.

Part 12 gives the fundamental properties of the alloys.

The following four ternary alloys are considered here: iron-chromium-aluminum alloy No.1, 16% - 18% Cr and 4.5 - 6.5% Al; alloy No.2, 23% - 27% Cr and 4.5% - 7% Al; alloy No.3, 40% 45% Cr and 7.5% - 12% Al; alloy No.4 65% - 68% Cr and 7.5% - 12.5% Al. All these alloys are located in the zone of ternary solid solution. Accordingly they possess a homogeneous ferritic structure.

Part 13 gives application of Fe-Cr-Al alloys.

Plants are now producing from No.1 and No.2 alloys hot rolled ribbons ~~2, 5~~ 2.5, 3, 3.5 and 4 mm. thick and wires of 5.5, 6, 7 and 8 mm thickness.

The cold drawn wires may be obtained as thin as 0.03 - 0.04 mm. in diam. Cold drawn ribbons of different thickness (up to 0.2mm) are produced. Electrical loadings permissible with No.1 and No.2 alloys are as follows: at temperatures up to 800°C permissible load is 1.6 to 1.8 watt/cm^2; at 1000°C,; 1.3 - 1.4 watt/cm^2; and at temperatures 1100°C and higher 0.8 - 1.0 watt/cm^2. The permissible loads are increasing

Approved For Release 2001/07/31 : CIA-RDP80-00809A000500170204-4

Approved For Release 2001/07/31 : CIA-RDP80-00809A000500170204-4

with an increase of heat resistance of alloys. Thus, for alloy No.2 they are higher than for alloy No.1, for alloy No.3 they are higher than with alloy No.2 and for alloy No.4 - higher than for alloy No.3.

BIBLIOGRAPHY pp. 185-189 - There are 210 references of which 70 refer to Russian authors.

Reviewer's remarks

This book should be of interest to American readers, particularly to those thoroughly familiar with the subject.

The book contains 51 tables and 154 figures. A great majority of them would require a lengthy description which is impossible to make in a short abstract. It is suggested, therefore, that the reader consults the text as indicated in the present review.

It is considered that magnification of some photomicrographs is not adequate; it is not high enough for a correct interpretation of the structures discussed.

Approved For Release 2001/07/31 : CIA-RDP80-00809A000500170204-4

Approved For Release 2001/07/31 : CIA-RDP80-00809A000500170204-4

25X1A

[redacted]

V. S. Doubovoi, "FLAKES IN STEEL" (Flokeni v Stali)

Government Scientific-Technical Publishing House of Ferrous and Non-Ferrous Metallurgy, Moscow, 1950.
Book 332 pages, divided into 7 parts.

PART I - CRITICAL ANALYSIS OF DIFFERENT THEORIES
pp 12-36

Various theories concerning the origin of internal fissure (flakes) which may occur in steel are reviewed. The gas bubbles, shrinkage cavities, high carbon, phosphorus or nitride segregations, non-metallic inclusions, internal stresses, or hydrogen are thought to be, by different authors, the principal cause of this phenomenon. All these theories are divided by the author into nine categories and the arguments for and against these theories are discussed. The author believes that none of the existing theories explain satisfactorily the origin of flakes. The most plausible explanation is the hydrogen theory. However, hydrogen does not seem to be the only factor promoting flakes. None of the existing theories can explain the fact that no flakes were observed in certain types of steel.

PART 2. EFFECT OF HYDROGEN ON FLAKE FORMATION
pp 37-91

Chapter 1 - Flake-sensitivity of steel. It has been established that flakes occur mostly in nickel, chromium, nickel-chromium, chromium-nickel-molybdenum, and some other alloy steels, i.e., steels of martensite and pearlitic types.

The "Electrosteel" plant made extensive investigations. According to the author's observations, the alloy martensitic steels are more prone to flaking than the alloyed pearlitic steels. In both cases the tendency to produce flakes increases with the increase in the carbon content. The

Approved For Release 2001/07/31 : CIA-RDP80-00809A000500170204-4

Approved For Release 2001/07/31 : CIA-RDP80-00809A000500170204-4

steels listed that have the greatest tendency to flake are chromium-nickel, chromium-nickel-molybdenum,-tungsten, and chromium-nickel-vanadium, in the high, medium, and low carbon types. The steels that flakes seldom occur are relatively the same except no tungsten is included and the carbon content varies between medium and low carbon types. The steels where no flakes were observed consists of the high speed tools steels and chromium type of stainless steels.

CHAPTER 2. INFLUENCE OF HYDROGEN ON THE FLAKE-SENSIVITY OF ALLOY STEELS, pp 37-90

18 heats of nickel-chromium-molybdenum steels and 2 chromium steels were made in different plants using the basic arc and high frequency induction electric furnaces. The molten bath was treated with different amounts of hydrogen which was introduced into the melt by blowing it through the molten metal or by blowing steam into the furnace atmosphere. Temperatures were measured with Pt/PtRh thermocouples. Chemical analysis were determined on samples of molten metal taken before pouring into the ladle. Steel ingots were hot forged or rolled and cut into sections. These sections (samples) were then cooled at different cooling rate. Some samples were cooled in slag cotton (wool), whilst others were air-cooled or cooled in warm water. (The results of these tests are given in Table 6). The alloy steels containing 0.00048 to 0.00063% hydrogen and cooled at 3 different cooling rates didn't show any flakes, whereas alloy steels containing higher amounts of hydrogen and cooled in air or warm water flaked. No flakes were observed in any steels cooled in slag cotton (wool). However, the author states, these results do not entirely prove that hydrogen is the sole factor responsible for flake formation in steel. The structural transformations taking place during air or water

Approved For Release 2001/07/31 : CIA-RDP80-00809A000500170204-4

Approved For Release 2001/07/31 : CIA-RDP80-00809A000500170204-4

cooling of steel samples produce stresses which in turn may be responsible for flake formation.

CHAPTER 3- EFFECT OF HYDROGEN ON THE FLAKE-SENSIVITY OF PLAIN CARBON STEEL pp 91-152

There were five plain carbon steels investigated. The carbon content of these steels varied between 0.47% and 1.01%. Each melt was treated with hydrogen. During the first period of melting a tiny stream of water was run into the furnace and then (period of refining) hydrogen was blown through the melt. (Results of gas analysis and temperatures of the molten metal, as measured by Pt/PtRh thermocouple at the time of taking samples, are given in Table II. The temperatures are shown in the last column, while in the preceding column are given the percents (weight) of the total hydrogen content in the molten metal.) The ingots from these melts were hot forged or rolled and sectioned into samples. Different rates of cooling of these samples were used, the samples being cooled in slag cotton (wool), in air, or warm water. The samples cooled in slag cotton (wool) were free from flakes, whereas all samples cooled in air and warm water exhibited flakes. Most flakes were observed in the water cooled samples. The number of flakes increased with an increase in the carbon content. The flake length of air and water-cooled steels were 0.6 to 2.1 mm., the maximum length being 8.3 mm. The flake length in the air-cooled samples increased with an increase in carbon. The following conclusions were drawn by the author from the above experiments: 1. The low manganese ($\leq$ 0.40%) and low silicon ($\leq$ 0.32%) steels may show flakes. 2. The hydrogen is the factor responsible for flake formation. 3. By regulating the rate of cooling it is possible to produce steel free from flakes. It may be assumed that during slow cooling a portion of hydrogen is removed, the

Approved For Release 2001/07/31 : CIA-RDP80-00809A000500170204-4

Approved For Release 2001/07/31 : CIA-RDP80-00809A000500170204-4

remaining portion being too small to promote flake formation. The size and arrangement of flakes in the water cooled samples were quite different from those cooled in air. This phenomenon cannot be explained only by the hydrogen theory. Evidently we are here dealing with some other factor besides hydrogen. According to the author, this factor results from the internal stresses produced by different cooling rates of the inner and outer zones of the sample and subsequent ununiformity in structure. The arrangement of quenching cracks and flakes on the cross-sections of samples indicated that maximum stresses were located in radial directions.

PART 3. THE MOMENT AT WHICH FLAKES ARE FORMED pp 90-152

The hypotheses advanced on this subject by various Russian and foreign investigators are reviewed. In order to establish the exact time at which flakes are formed steel ingots of nine heats were investigated by the author. All these heats were treated with hydrogen by blowing it through the melt. The ingots were forged into square bars having sides of 85 to 90 mm. and sectioned into samples 250 mm. long. At the end of the forging operation the temperature of the forged bars were 1000°-1020°C.

1st series of Tests: For cooling the nickel-chromium-molybdenum steel some of the samples were placed vertically on the sand floor while other samples were put on the metal floor. The minimum distance between samples was 1 meter. They were cooled to a temperature of 30°C in this position. The average cooling rate for the interval 900° to 30°C was 2°C per minute for the first group and 4°C per min. for the second. These samples then were subjected to aging at room temperature for different periods - 0,1,4,8,12,16,24,48,72,96 and 360 hours; for the second group of

Approved For Release 2001/07/31 : CIA-RDP80-00809A000500170204-4

Approved For Release 2001/07/31 : CIA-RDP80-00809A000500170204-4

the maximum length of the aging time was 720 hours. The aged samples were placed in the annealing furnace and held there at 650°C for 16 hours. After this operation they were placed in slag cotton (wool) and cooled to 150°C. Afterwards, samples were put again into the furnace, and slowly heated to 860°C and held at this temperature for 4 hours. Again they were cooled in the slag cotton to 150°C, then tempered at 650°C for 16 hours and finally cooled to room temperature.

2nd series of tests: Some specimens of this series were air cooled to 300°, 200°, and 100°C, placed into slag cotton and cooled to 30°C. Next, they were tempered at 650°C for 16 hours and slag-cotton cooled. Other specimens were cooled in boiling water and then in cool water (30°C). One half of these samples were heated at 650°C for 16 hours and cotton-cooled to 30°C. The others were aged at room temperature for 360 hours and tempered at 650°C. In addition to the foregoing experiments, one sample from each heat was cooled after forging in slag-cotton to 30°C, the cooling rates being 15° - 16°C per hour in the interval 750° - 450°C and 5° - 8°C per hour in the interval 450° - 150°C. The cooled samples were aged for 360 hours in air, tempered at 650° for 16 hours and slag-cotton cooled.

3rd series of tests: The specimens from the first group of heats after forging were air cooled to 300°, 200°, and 100°C and specimens from one of the second group of heats were air cooled to 200°, 150° and 100°C. They were then aged at those temperatures for 1, 4, 8, 12, 16, 20, and 24 hours. One sample of each of the above groups was air cooled to 30°C and aged at room temperature for 360 hours. The second sample taken from the above groups was heated at 650°C for 16 hours, slag-cotton cooled for 16 hours and aged at room temperature for 360 hours. In summarizing the

Approved For Release 2001/07/31 : CIA-RDP80-00809A000500170204-4

Approved For Release 2001/07/31 : CIA-RDP80-00809A000500170204-4

results of these tests, the following conclusions were drawn by the author: 1. The moment of flake-formation depends upon the chemical analysis, rate of cooling and degree of flake sensitivity of the steel. With an increase of nickel, manganese, chromium and probably some other alloying elements, the flake-sensitivity increases. At the same time the flake formation moment occurs at lower temperatures. An increase in the carbon content also increases flake-sensitivity of steel, but the moment of flake formation is shifted towards higher temperatures. As the cooling rate increases, the flake-sensitivity of the steel increases and the flake-formation moment is shifted towards lower temperatures. 2. In chromium-nickel-molybdenum steel no flakes are formed at 150°C and higher temperatures and in chromium steels at temperature of 250°C and higher. 3. Depending upon the cooling rate of steel after hot working, flakes may be not formed at all, or may be formed during cooling or aging at room temperature. 4. The flake formation proceeds gradually. At first fine flakes make their appearance. With further cooling the flakes increase in size and number. Flake formation may last for very many hours, particularly in the high alloy steels, possessing high plastic properties.

PART 4 - PREVENTING OF FLAKES FORMATION BY HEAT-TREATMENT
pp 153-253)

Some investigators came to the conclusion that holding at temperatures above AC, has no effect on the flake-sensitivity of steel. The author does not agree with this and states that his experiments demonstrated that an immunity to flake-sensitivity may be obtained by an isothermal holding of the forged steel for a definite period of time depending upon the chemical composition and temperature. It has been established by the

Approved For Release 2001/07/31 : CIA-RDP80-00809A000500170204-4

Approved For Release 2001/07/31 : CIA-RDP80-00809A000500170204-4

author that isothermal holding has an effect on preventing the flake formation in the chromium-nickel-molybdenum steel within the temperature interval 150° to 1150°C and in the chromium steel within 250° to 1000°C. It may be pointed out that the grains of chromium-nickel-molybdenum and chromium steels become very large at temperatures of 1150°C and 1000°C respectively. We also know that with an increase in grain size the plastic properties of steel are lowered and the flake-sensitivity, therefore, increases.

Of all the gases known which can dissolve in the ferrous alloys, hydrogen possesses the highest rate of diffusion. It is different for different structural phases of steel and is increasing with a temperature increase. It is known that in the case of alpha iron, hydrogen evolutions take place at high as well as at low temperatures, 200°, 100°, and even room temperature. However, at low temperatures this process proceeds slowly. There is practically no hydrogen evolution at low temperatures from gamma iron.

With a decrease in the hydrogen concentration in steel, the internal stresses become lower and the plastic properties higher. This, the author states, explains why the isothermic treatments (above and below AC), may prevent flake formation in steel.

PART 5 - EFFECT OF HYDROGEN ON MECHANICAL PROPERTIES OF STEEL

pp 254-270

With an increase in hydrogen the ultimate strength, impact toughness and particularly elongation and compression of steel decrease, whereas the proportional limit and yield point are raised. For certain hydrogen content, (different for different types of steel) the break occurs without any elongation ~~and~~ or formation of a neck. This phenomenon indicates a

Approved For Release 2001/07/31 : CIA-RDP80-00809A000500170204-4

Approved For Release 2001/07/31 : CIA-RDP80-00809A000500170204-4

complete loss of the plastic properties of steel.

PART 6 - NATURE OF FLAKES pp 271-293

It is well known that flakes quite often appear as sizeable areas of silvery brightness on the fracture of alloy steels. The fractures of samples of flaky steels are illustrated on figures 83 to 87 (pp 271-275).

On the basis of his observations, the author comes to conclusion that flakes are hair cracks.

Many investigations were conducted during the last several years on the weldability of flakes. The results obtained were discussed at length by a special committee of the Eastern Metallurgists. It was decided that flakes may be completely welded by hot rolling, but that the reductions used must vary according to the flakes arrangement and type of steel. One should remember, however, that welded flakes may appear again. Therefore, many plants remain suspicious on this matter.

PART 7 - FACTORS INFLUENCING THE DEVELOPMENT OF FLAKES AND MECHANISM OF THEIR FORMATION pp 294-327

Different factors which may promote flake development are considered. These factors are: non-metallic inclusions, mechanical stresses, thermal stresses, structural stresses, and hydrogen. The author believes that hydrogen and structural stresses are the two principal factors responsible for flake formation.

Bibliography (pp. 328-331) There are 72 items of which 40 refer to Russian publications.

Reviewer's remarks: This book is difficult to read on account of an excessive number of details which are not well coordinated. The arguments against the hydrogen theory (that hydrogen is the only factor responsible for

Approved For Release 2001/07/31 : CIA-RDP80-00809A000500170204-4

Approved For Release 2001/07/31 : CIA-RDP80-00809A000500170204-4

the presence of flakes) are somewhat conflicting and not entirely convincing. However, some data presented by the author and described in this review should be of interest to American readers.

25X1X

[redacted]
January 5, 1953

Approved For Release 2001/07/31 : CIA-RDP80-00809A000500170204-4